Berkel S, Marshall CR, Weiss B, Howe J, Roeth R, Moog U, Endris V, Roberts W, Szatmari P, Pinto D, Bonin M, Riess A, Engels H, Sprengel R, Scherer SW, Rappold GA. 2010. Mutations in the SHANK2 synaptic scaffolding gene in autism spectrum disorder and mental retardation. Nat Genet 42:489–491.

Bonora E, Lamb JA, Barnby G, Sykes N, Moberly T, Beyer KS, Klauck SM, Poustka F, Bacchelli E, Blasi F, Maestrini E, Battaglia A, Haracopos D, Pedersen L, Isager T, Eriksen G, Viskum B, Sorensen EU, Brondum-Nielsen K, Cotterill R, Engeland H, Jonge M, Kemner C, Steggehuis K, Scherpenisse M, Rutter M, Bolton PF, Parr JR, Poustka A, Bailey AJ, Monaco AP, International Molecular Genetic Study of Austism Consortium. 2005. Mutation screening and association analysis of six candidate genes for autism on chromosome 7q. Eur J Hum Genet 13:198–207.

Cisternas FA, Vincent JB, Scherer SW, Ray PN. 2003. Cloning and characterization of human CADPS and CADPS2, new members of the Ca^{2+}-dependent activator for secretion protein family. Genomics 81: 279–291.

Cukier HN, Skaar DA, Rayner-Evans MY, Konidari I, Whitehead PL, Jaworski JM, Cuccaro ML, Pericak-Vance MA, Gilbert JR. 2009. Identification of chromosome 7 inversion breakpoints in an autistic family narrows candidate region for autism susceptibility. Autism Res 2: 258–266.

Dauwerse JG, Ruivenkamp CA, Hansson K, Marijnissen GM, Peters DJ, Breuning MH, Hilhorst-Hofstee Y. 2010. A complex chromosome 7q rearrangement identified in a patient with mental retardation, anxiety disorder, and autistic features. Am J Med Genet Part A 152A:427–433.

Durand CM, Betancur C, Boeckers TM, Bockmann J, Chaste P, Fauchereau F, Nygren G, Rastam M, Gillberg IC, Anckarsäter H, Sponheim E, Goubran-Botros H, Delorme R, Chabane N, Mouren-Simeoni MC, de Mas P, Bieth E, Rogé B, Héron D, Burglen L, Gillberg C, Leboyer M, Bourgeron T. 2007. Mutations in the gene encoding the synaptic scaffolding protein SHANK3 are associated with autism spectrum disorders. Nat Genet 39:25–27.

Eran A, Graham KR, Vatalaro K, McCarthy J, Collins C, Peters H, Brewster SJ, Hanson E, Hundley R, Rappaport L, Holm IA, Kohane IS, Kunkel LM. 2009. Comment on "Autistic-like phenotypes in Cadps2-knockout mice and aberrant CADPS2 splicing in autistic patients". J Clin Invest 119: 679–680.

Glessner JT, Wang K, Cai G, Korvatska O, Kim CE, Wood S, Zhang H, Estes A, Brune CW, Bradfield JP, Imielinski M, Frackelton EC, Reichert J, Crawford EL, Munson J, Sleiman PM, Chiavacci R, Annaiah K, Thomas K, Hou C, Glaberson W, Flory J, Otieno F, Garris M, Soorya L, Klei L, Piven J, Meyer KJ, Anagnostou E, Sakurai T, Game RM, Rudd DS, Zurawiecki D, McDougle CJ, Davis LK, Miller J, Posey DJ, Michaels S, Kolevzon A, Silverman JM, Bernier R, Levy SE, Schultz RT, Dawson G, Owley T, McMahon WM, Wassink TH, Sweeney JA, Nurnberger JI, Coon H, Sutcliffe JS, Minshew NJ, Grant SF, Bucan M, Cook EH, Buxbaum JD, Devlin B, Schellenberg GD, Hakonarson H. 2009. Autism genome-wide copy number variation reveals ubiquitin and neuronal genes. Nature 459:569–573.

International Molecular Genetic Study of Autism Consortium. 1998. A full genome screen for autism with evidence for linkage to a region on chromosome 7q. Hum Mol Genet 7:571–578.

International Molecular Genetic Study of Autism Consortium (IMGSAC). 2001. Further characterization of the autism susceptibility locus AUTS1 on chromosome 7q. Hum Mol Genet 10:973–982.

Jamain S, Quach H, Betancur C, Råstam M, Colineaux C, Gillberg IC, Soderstrom H, Giros B, Leboyer M, Gillberg C, Bourgeron T. Paris Autism Research International Sibpair Study. 2003. Mutations of the X-linked genes encoding neuroligins NLGN3 and NLGN4 are associated with autism. Nat Genet 34:27–29.

Junge HJ, Yang S, Burton JB, Paes K, Shu X, French DM, Costa M, Rice DS, Ye W. 2009. TSPAN12 regulates retinal vascular development by promoting Norrin- but not Wnt-induced FZD4/beta-catenin signaling. Cell 139:299–311.

Kim HG, Kishikawa S, Higgins AW, Seong IS, Donovan DJ, Shen Y, Lally E, Weiss LA, Najm J, Kutsche K, Descartes M, Holt L, Braddock S, Troxell R, Kaplan L, Volkmar F, Klin A, Tsatsanis K, Harris DJ, Noens I, Pauls DL, Daly MJ, MacDonald ME, Morton CC, Quade BJ, Gusella JF. 2008. Disruption of neurexin 1 associated with autism spectrum disorder. Am J Hum Genet 82:199–207.

Lennon PA, Cooper ML, Peiffer DA, Gunderson KL, Patel A, Peters S, Cheung SW, Bacino CA. 2007. Deletion of 7q31.1 supports involvement of FOXP2 in language impairment: Clinical report and review. Am J Med Genet A 143A:791–798.

Marshall CR, Noor A, Vincent JB, Lionel AC, Feuk L, Skaug J, Shago M, Moessner R, Pinto D, Ren Y, Thiruvahindrapduram B, Fiebig A, Schreiber S, Friedman J, Ketelaars CE, Vos YJ, Ficicioglu C, Kirkpatrick S, Nicolson R, Sloman L, Summers A, Gibbons CA, Teebi A, Chitayat D, Weksberg R, Thompson A, Vardy C, Crosbie V, Luscombe S, Baatjes R, Zwaigenbaum L, Roberts W, Fernandez B, Szatmari P, Scherer SW. 2008. Structural variation of chromosomes in autism spectrum disorder. Am J Hum Genet 82:477–488.

Miller DT, Adam MP, Aradhya S, Biesecker LG, Brothman AR, Carter NP, Church DM, Crolla JA, Eichler EE, Epstein CJ, Faucett WA, Feuk L, Friedman JM, Hamosh A, Jackson L, Kaminsky EB, Kok K, Krantz ID, Kuhn RM, Lee C, Ostell JM, Rosenberg C, Scherer SW, Spinner NB, Stavropoulos DJ, Tepperberg JH, Thorland EC, Vermeesch JR, Waggoner DJ, Watson MS, Martin CL, Ledbetter DH. 2010. Consensus statement: Chromosomal microarray is a first-tier clinical diagnostic test for individuals with developmental disabilities or congenital anomalies. Am J Hum Genet 86:749–764.

Moessner R, Marshall CR, Sutcliffe JS, Skaug J, Pinto D, Vincent J, Zwaigenbaum L, Fernandez B, Roberts W, Szatmari P, Scherer SW. 2007. Contribution of SHANK3 mutations to autism spectrum disorder. Am J Hum Genet 81:1289–1297.

Nikopoulos K, Gilissen C, Hoischen A, van Nouhuys CE, Boonstra FN, Blokland EA, Arts P, Wieskamp N, Strom TM, Ayuso C, Tilanus MA, Bouwhuis S, Mukhopadhyay A, Scheffer H, Hoefsloot LH, Veltman JA, Cremers FP, Collin RW. 2010. Next-generation sequencing of a 40 Mb linkage interval reveals TSPAN12 mutations in patients with familial exudative vitreoretinopathy. Am J Hum Genet 86:240–247.

Poulter JA, Ali M, Gilmour DF, Rice A, Kondo H, Hayashi K, Mackey DA, Kearns LS, Ruddle JB, Craig JE, Pierce EA, Downey LM, Mohamed MD, Markham AF, Inglehearn CF, Toomes C. 2010. Mutations in TSPAN12 cause autosomal-dominant familial exudative vitreoretinopathy. Am J Hum Genet 86:248–253.

Sadakata T, Washida M, Iwayama Y, Shoji S, Sato Y, Ohkura T, Katoh-Semba R, Nakajima M, Sekine Y, Tanaka M, Nakamura K, Iwata Y, Tsuchiya KJ, Mori N, Detera-Wadleigh SD, Ichikawa H, Itohara S, Yoshikawa T, Furuichi T. 2007a. Autistic-like phenotypes in Cadps2-knockout mice and aberrant CADPS2 splicing in autistic patients. J Clin Invest 117:931–943.

Sadakata T, Kakegawa W, Mizoguchi A, Washida M, Katoh-Semba R, Shutoh F, Okamoto T, Nakashima H, Kimura K, Tanaka M, Sekine Y, Itohara S, Yuzaki M, Nagao S, Furuichi T. 2007b. Impaired cerebellar development and function in mice lacking CAPS2, a protein involved in neurotrophin release. J Neurosci 27:2472–2482.

Sadakata T, Washida M, Furuichi T. 2007c. Alternative splicing variations in mouse CAP S2: Differential expression and functional properties of splicing variants. BMC Neurosci 8:25.

Sebat J, Lakshmi B, Malhotra D, Troge J, Lese-Martin C, Walsh T, Yamrom B, Yoon S, Krasnitz A, Kendall J, Leotta A, Pai D, Zhang R, Lee YH, Hicks

J, Spence SJ, Lee AT, Puura K, Lehtimäki T, Ledbetter D, Gregersen PK, Bregman J, Sutcliffe JS, Jobanputra V, Chung W, Warburton D, King MC, Skuse D, Geschwind DH, Gilliam TC, Ye K, Wigler M. 2007. Strong association of de novo copy number mutations with autism. Science 316:445–449.

Shastry BS. 2009. Persistent hyperplastic primary vitreous: Congenital malformation of the eye. Clin Experiment Ophthalmol 37:884–890.

Shen Y, Dies KA, Holm IA, Bridgemohan C, Sobeih MM, Caronna EB, Miller KJ, Frazier JA, Silverstein I, Picker J, Weissman L, Raffalli P, Jeste S, Demmer LA, Peters HK, Brewster SJ, Kowalczyk SJ, Rosen-Sheidley B, McGowan C, Duda AW III, Lincoln SA, Lowe KR, Schonwald A, Robbins M, Hisama F, Wolff R, Becker R, Nasir R, Urion DK, Milunsky JM, Rappaport L, Gusella JF, Walsh CA, Wu BL, Miller DT. Autism Consortium Clinical Genetics/DNA Diagnostics Collaboration. 2010. Clinical genetic testing for patients with autism spectrum disorders. Pediatrics 125:e727–e735.

Shimojima K, Páez MT, Kurosawa K, Yamamoto T. 2009. Proximal interstitial 1p36 deletion syndrome: The most proximal 3.5-Mb microdeletion identified on a dysmorphic and mentally retarded patient with inv(3)(p14.1q26.2). Brain Development 31:629–633.

Singh B, Ogiwara I, Kaneda M, Tokonami N, Mazaki E, Baba K, Matsuda K, Inoue Y, Yamakawa K. 2006. A Kv4.2 truncation mutation in a patient with temporal lobe epilepsy. Neurobiol Dis 24:245–253.

Ye X, Wang Y, Nathans J. 2010. The Norrin/Frizzled4 signaling pathway in retinal vascular development and disease. Trends Mol Med 16:417–425.

RESEARCH ARTICLE

AMERICAN JOURNAL OF medical genetics PART A

Delineation of Dermatan 4-*O*-sulfotransferase 1 Deficient Ehlers–Danlos Syndrome: Observation of Two Additional Patients and Comprehensive Review of 20 Reported Patients

Kenji Shimizu,[1] Nobuhiko Okamoto,[2] Noriko Miyake,[3] Katsuaki Taira,[4] Yumiko Sato,[5] Keiko Matsuda,[2] Noriko Akimaru,[2] Hirofumi Ohashi,[1] Keiko Wakui,[6] Yoshimitsu Fukushima,[6] Naomichi Matsumoto,[3] and Tomoki Kosho[6]*

[1]Division of Medical Genetics, Saitama Children's Medical Center, Saitama, Japan

[2]Department of Medical Genetics, Osaka Medical Center and Research Institute for Maternal and Child Health, Osaka, Japan

[3]Department of Human Genetics, Yokohama City University Graduate School of Medicine, Yokohama, Japan

[4]Department of Orthopedics, Saitama Children's Medical Center, Saitama, Japan

[5]Department of Radiology, Saitama Children's Medical Center, Saitama, Japan

[6]Department of Medical Genetics, Shinshu University School of Medicine, Matsumoto, Japan

Received 20 January 2011; Accepted 21 April 2011

Loss-of-function mutations in *CHST14*, dermatan 4-*O*-sulfotransferase 1 (D4ST1) deficiency, have recently been found to cause adducted thumb-clubfoot syndrome (ATCS; OMIM-#601776) and a new type of Ehlers–Danlos syndrome (EDS) coined as EDS Kosho Type (EDSKT) [Miyake et al., 2010], as well as a subset of kyphoscoliosis type EDS without lysyl hydroxylase deficiency (EDS VIB) coined as musculocontractural EDS (MCEDS) [Malfait et al., 2010]. Lack of detailed clinical information from later childhood to adulthood in ATCS and lack of detailed clinical information from birth to early childhood in EDSKT and MCEDS have made it difficult to determine whether these disorders would be distinct clinical entities or a single clinical entity with variable expressions and with different presentations depending on the patients' ages at diagnosis. We present detailed clinical findings and courses of two additional unrelated patients, aged 2 years and 6 years, with EDSKT with a comprehensive review of 20 reported patients with D4ST1 deficiency, which supports the notion that these disorders constitute a clinically recognizable form of EDS. The disorder, preferably termed D4ST1-deficient EDS, is characterized by progressive multisystem fragility-related manifestations (joint dislocations and deformities, skin hyperextensibility, bruisability, and fragility; recurrent large subcutaneous hematomas, and other cardiac valvular, respiratory, gastrointestinal, and ophthalmological complications) resulting from impaired assembly of collagen fibrils, as well as various malformations (distinct craniofacial features, multiple congenital contractures, and congenital defects in cardiovascular, gastrointestinal, renal, ocular, and central nervous systems) resulting from inborn errors of development.

How to Cite this Article:
Shimizu K, Okamoto N, Miyake N, Taira K, Sato Y, Matsuda K, Akimaru N, Ohashi H, Wakui K, Fukushima Y, Matsumoto N, Kosho T. 2011. Delineation of Dermatan 4-*O*-sulfotransferase 1 Deficient Ehlers–Danlos Syndrome: Observation of Two Additional Patients and Comprehensive Review of 20 Reported Patients.
Am J Med Genet Part A.

Key words: dermatan 4-*O*-sulfotransferase 1 deficiency; adducted thumb-clubfoot syndrome; Ehlers–Danlos syndrome Kosho type; musculocontractural Ehlers–Danlos syndrome; congenital contractures; progressive multisystem fragility-related manifestations; malformations

Additional supporting information may be found in the online version of this article.
Grant sponsor: Research on Intractable Diseases, Ministry of Health, Labor and Welfare, Japan; Grant number: 2141039040.
Kenji Shimizu, Nobuhiko Okamoto, and Tomoki Kosho have equally contributed to this work.
*Correspondence to:
Tomoki Kosho, MD, Department of Medical Genetics, Shinshu University School of Medicine, 3-1-1 Asahi, Matsumoto 390-8621, Japan.
E-mail: ktomoki@shinshu-u.ac.jp
Published online 00 Month 2011 in Wiley Online Library (wileyonlinelibrary.com).
DOI 10.1002/ajmg.a.34115

INTRODUCTION

Dermatan 4-*O*-sulfotransferase 1 (D4ST1) is a regulatory enzyme in the glycosaminoglycan biosynthesis that transfers active sulfate to position 4 of the *N*-acetyl-D-galactosamine residues of dermatan sulfate [Evers et al., 2001; Mikami et al., 2003]. Dermatan sulfate, as well as chondroitin sulfate and heparan sulfate, constitutes glycosaminoglycan sidechains of proteoglycans; and has been implicated in cardiovascular disease, tumorigenesis, infection, wound repair, and fibrosis via dermatan sulfate-containing proteoglycans such as decorin and biglycan [Trowbridge and Gallo, 2002]. Carbohydrate sulfotransferase 14 (*CHST14*), localized on 15q12, is the gene encoding D4ST1. Recently, loss-of-function mutations in *CHST14* (D4ST1 deficiency) have been found to cause adducted thumb-clubfoot syndrome (ATCS; OMIM#601776) in 11 patients from four families [Dündar et al., 2009] and a variant of Ehlers–Danlos syndrome (EDS) in six patients from six families [Miyake et al., 2010], tentatively coined as EDS Kosho Type (EDSKT) in the London Dysmorphology Database (http://www.lmdatabases.com/index.html) and POSSUM (http://www.possum.net.au/). ATCS was originally recognized as a new type of arthrogryposis, focused on characteristic clinical pictures from birth to early childhood, including adducted thumbs and talipes equinovarus as well as facial dysmorphisms (prominent forehead, large fontanelle, hypertelorism, down-slanting palpebral fissures, low-set ears), and arachnodactyly [Dündar et al., 1997; Sonoda and Kouno, 2000; Dündar et al., 2001; Janecke et al., 2001]. In a recent study by Dündar et al. [2009], ATCS has been categorized again as a connective tissue disorder, based on additional clinical pictures from childhood to adolescence, including skin fragility and bruisability, joint laxity, and osteopenia. EDSKT comprises a pattern of distinct craniofacial features, multiple congenital contractures, progressive joint and skin laxity, and progressive multisystem fragility-related manifestations, including recurrent large subcutaneous hematomas and other cardiac, respiratory, gastrointestinal, ophthalmological complications [Yasui et al., 2003; Kosho et al., 2005, 2010].

Very recently, Malfait et al. [2010] have independently found mutations in *CHST14* in three patients from two families, who were diagnosed with kyphoscoliosis type EDS without lysyl hydroxylase deficiency (EDS VIB). They concluded that their series and ATCS, as well as EDSKT, formed a phenotypic continuum based on their clinical observations and identification of an identical mutation in both conditions, and proposed to coin the disorder as "musculocontractural EDS" (MCEDS) [Malfait et al., 2010]. However, it is still an unsolved problem whether ATCS, EDSKT, and MCEDS would be distinct clinical entities or a single clinical entity with variable inter- and intrafamilial expressions and with different presentations depending on the patients' ages at diagnosis [Miyake et al., 2010], because detailed clinical information are lacking in ATCS from later childhood to adulthood and in EDSKT and MCEDS from birth to early childhood.

Here, we present detailed clinical findings and courses of two additional unrelated patients, aged 2 years and 6 years, with EDSKT, which would contribute to delineate comprehensive phenotypic spectrum of D4ST1 deficiency.

CLINICAL REPORTS

Patient 1

The patient, a Japanese boy, was the second child of a healthy 31-year-old mother and a healthy 33-year-old nonconsanguineous father. He was born by cesarean for breech presentation at 38 weeks and 3 days of gestation. His birth weight was 3,092 g (+0.2 SD), length 46 cm (−1.3 SD), and OFC 34 cm (+0.4 SD). At age 15 days, he was referred to our hospital for the treatment of bilateral talipes equinovarus. He had a round face with a large fontanelle, hypertelorism, short palpebral fissures, blue sclerae, strabismus, a short nose with a hypoplastic columella, low-set and rotated ears, a high palate, a long philtrum, a thin upper lip vermillion, a small mouth, and microretrognathia (Fig. 1A, B). He had arachnodactyly, flexion-adduction contractures of bilateral thumbs, flexion contractures of the interphalangeal (IP) joints in the other fingers, flexion contractures of bilateral elbows and knees, and rigidity of bilateral hip joints (Fig. 1C). He also had widely spaced nipples, a redundant and translucent skin, an umbilical hernia, and bilateral cryptorchidism (Fig. 1C). Talipes equinovarus was treated with incision of bilateral Achilles' tendons at age 2 months, followed by serial plaster casts and braces. Skin fragility was observed at the procedure. It was surgically corrected at age 1 year and 11 months. Gross motor development was delayed: He raised his head at 6 months, sat without support at age 1 year, stood up assisted at age 1 year and 6 months, and walked assisted after surgical correction of talipes equinovarus. He had bruises easily on the occiput

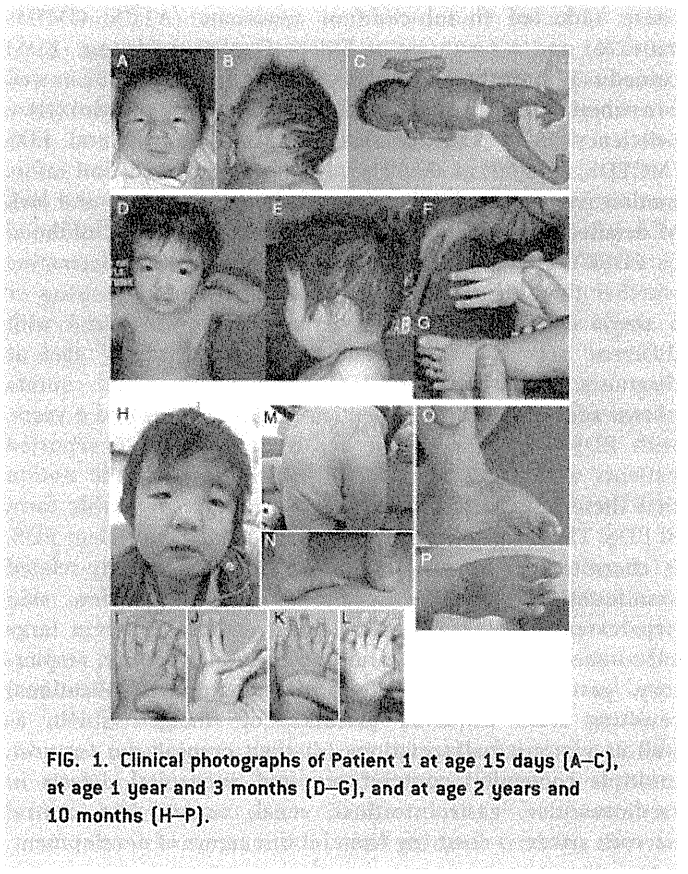

FIG. 1. Clinical photographs of Patient 1 at age 15 days (A–C), at age 1 year and 3 months (D–G), and at age 2 years and 10 months (H–P).

and buttocks after falling, which were absorbed spontaneously. Bleeding time was 1.3 min (normal values, 1–5 min), prothrombin time-international normalized ratio (PT-INR) 1.00 (normal values, 0.81–1.38 sec), and activated partial thromboplastin time (APTT) 27.9 sec (normal values, 23–36 sec).

When seen by us at age 1 year and 3 months, his craniofacial shape became square with a broad, bossed forehead, and hypertelorism with downslanting palpebral fissures became evident (Fig. 1D, E). Skin redundancy and tapering fingers and toes were noted (Fig. 1D, F, G). Ear rotation and flexion contractures of fingers improved (Fig. 1E, F).

When last seen by us at age 2 years and 10 months, he weighed 9.86 kg (−2.4 SD), height 84.9 cm (−2.1 SD), and OFC 45.5 cm (−2.4 SD). His face was slender, and was characterized by an unclosed fontanelle, hypertelorism, short and downslanting palpebral fissures, blue sclerae, strabismus, a short nose with a hypoplastic columella, low-set ears, a high palate, a long philtrum, a thin upper lip vermillion, a small mouth, and microretrognathia (Fig. 1H). He had a Marfanoid habitus, generalized joint laxity, a flat and thin thorax, and distinctive fingers (tapering with enlargement of distal phalanges) (Fig. 1I–L), and talipes valgus and planus with extremely soft subcutaneous tissues at the heels (Fig. 1N–P). The distal IP joints in bilateral index to little fingers and the IP/metacarpophalangeal (MP) joints in bilateral thumbs could hardly be flexed or extended. The MP joints in bilateral index to little fingers could be moved with poor flexion and hyperextension (see Supplementary Video 1 online). He had hyperextensible to redundant skin with bruisability and fine palmer creases (Fig. 1J, L, M). He suffered from constipation (defecation twice a week), treated with oral magnesium oxide. Ophthalmological examinations showed mild esotropia, and amblyopia due to severe hyperopic astigmatism. A cardiac ultrasonography showed no defects or valve abnormalities but mild dilation of the ascending aorta at the sinus of Valsalva. A brain CT showed no ventricular enlargement (Fig. 3O, P). G-banded chromosomes were normal. The Kinder Infant Developmental Scale [Cheng et al., 2010] showed mild developmental delay with the overall developmental quotient as 65 (physical/motor, 35; manipulation, 58; receptive language, 77; expressive language, 103; conceptual thinking, 77; social relationships with children, 68; social relationships with adults, 116; home training, 68; feeding, 42). He had orchiopexy and a surgical correction of an umbilical hernia at age 2 years and 7 months.

Patient 2

The patient, a Japanese boy, was the first child of a healthy 25-year-old mother and a healthy 28-year-old nonconsanguineous father. He was born by normal vaginal delivery at 38 weeks of gestation. His birth weight was 2940 g (+0.3 SD), length 49.1 cm (+0.3 SD), and OFC 32 cm (−0.5 SD). He was admitted for the treatment of bilateral adducted thumbs and talipes equinovarus. His craniofacial features included a large fontanelle, a high forehead, hypertelorism, short and downslanting palpebral fissures, blue sclerae, strabismus, a short nose with a hypoplastic columella, low-set and rotated ears, a high palate, a long philtrum, a thin upper lip vermillion, a small mouth, and microretrognathia (Fig. 2A). He had arachnodactyly, flexion-adduction contractures of bilateral thumbs, flexion contractures of the IP joints in the other fingers, rigidity of bilateral hip joints, and mild pectus excavatum (Fig. 2A, B). He also had widely spaced nipples, a redundant skin, and bilateral cryptorchidism (Fig. 2A). He suckled poorly and hated to be hugged tightly, suggesting hyperalgesia to pressure. Talipes equinovarus was treated with serial plaster casts. Gross motor development was delayed: He raised his head at 7 months, sat without support at age 1 year and 2 months, crawled at age 1 year and 6 months, pulled himself up by holding to something at age 1 year and 6 months, and walked unassisted at age 2 years and 6 months. His fontanelle was closed at age 3 years.

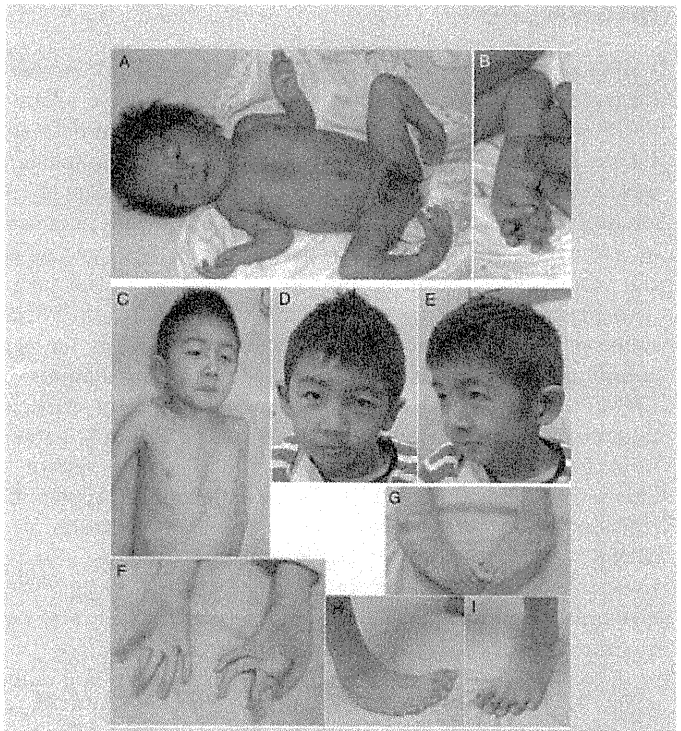

FIG. 2. Clinical photographs of Patient 2 at birth (A, B) and at age 6 years and 6 months (C–I).

At age 3 years, he developed a large subcutaneous hematoma over the skull after falling. Hematomas on the lower legs frequently occurred. He had recurrent dislocations of bilateral shoulders.

When last seen by us at age 6 years and 6 months, he weighed 16.4 kg (−1.4 SD), height 112 cm (−1.0 SD), and OFC 51.5 cm (−0.2 SD). He could jump unassisted. His craniofacial features included hypertelorism, short and downslanting palpebral fissures, blue sclerae, strabismus, a short nose with a hypoplastic columella, low-set ears, a high palate, a long philtrum, a thin upper lip vermillion, a small mouth, and microretrognathia (Fig. 2D, E). He had a Marfanoid habitus, generalized joint laxity, and pectus excavatum (Fig. 2C). His fingers were cylindrical and slender (Fig. 2F). He showed talipes equinovarus when lying down (Fig. 2G) and talipes planus when standing (Fig. 2H, I). The subcutaneous tissues at the heels were extremely soft. The distal IP joints in bilateral index to little fingers and the IP joints in bilateral thumbs

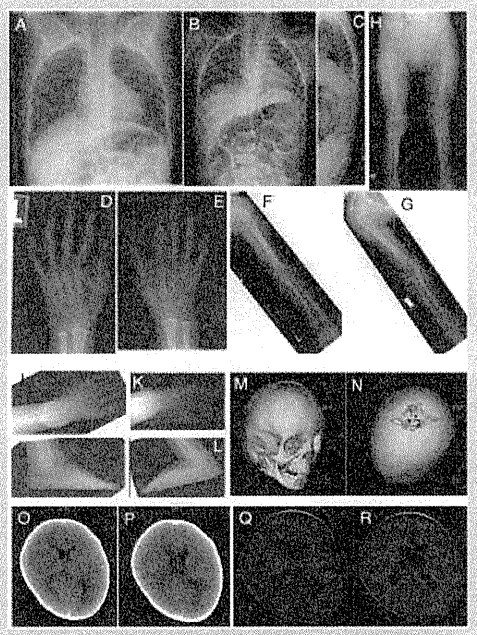

FIG. 3. Radiographs of Patient 1 at age 1 year and 10 months (A) and 2 years and 6 months (B–L). Cranial and brain CT of Patient 1 at age 2 years and 6 months (M–P). Brain MRI of Patient 2 at age 1 year and 10 months (Q, R).

could hardly be flexed or extended. The proximal IP joints in bilateral index to little fingers and the MP joints in all fingers could be flexed and extended, but could not be moved separately and smoothly. His skin was hyperextensible and bruisable. Fine palmar creases were also noted (Fig. 2F). He occasionally had constipation and abdominal pain. A cardiac ultrasonography showed trivial mitral valve prolapse, patent ductus arteriosus, and dextrocardia. A brain MRI showed bilateral ventricular enlargement (Fig. 3Q, R). G-banded chromosomes were normal. His intelligence was normal.

SKELETAL INVESTIGATIONS

Radiographs of Patient 1 were reviewed. At age 2 years and 6 months, he had mild scoliosis (Fig. 3B), which was not noted at age 1 year and 10 months (Fig. 3A). Physiological lumbar lordosis was not present (Fig. 3C). The left hip joint was dislocated (Fig. 3H). Long bones of the legs and arms showed over modeling, with narrowing diaphysis and widening metaphysis (Fig. 3F–H). Bilateral tibiae and fibulae were medially curved (Fig. 3H). Short bones of the hands (Fig. 3D, E) and feet (Fig. 3I–L) also showed over modeling, as well as osteoporotic changes in the feet (Fig. 3I–L).

MUTATION ANALYSIS

Genomic DNA was extracted from peripheral blood leukocytes of the patients and their parents, and was amplified with PCR using four primer sets for *CHST14* (sequences available on request). Through direct sequencing of the PCR products, compound heterozygous mutations were detected in both patients: c.842 C > T causing p. Pro281Leu (p.P281L) and c.878 A > G causing p.Tyr293Cys (p.Y293C) in Patient 1; c.626 T > C causing p.Phe209Ser (p.F209S) and c.842 C > T causing p.Pro281Leu (p.Y293C) in Patient 2 (data not shown). The parents had one of the two heterozygous mutations observed in their children.

DISCUSSION

We have presented detailed clinical characteristics and courses of two new unrelated pediatric patients with compound heterozygous *CHST14* mutations. The features showed striking resemblance to those of patients with EDSKT in their infancy to early childhood [Kosho et al., 2005, 2010]. *CHST14* mutations (P281L/Y293C) in Patient 1 were identical to those found in two patients with EDSKT [Miyake et al., 2010]. F209S found in Patient 2, which was not listed on a database of common gene variations in the Japanese population (JSNP) [Haga et al., 2002], was the mutation that has never found in previous patients with ATCS, EDSKT, or MCEDS.

To date, 22 patients (12 males, 10 females) from 14 families, including present patients, have been reported to have homozygous or compound heterozygous mutations in *CHST14* (Tables I and II) [Dündar et al., 1997; Sonoda and Kouno, 2000; Dündar et al., 2001; Janecke et al., 2001; Yasui et al., 2003; Kosho et al., 2005; Dündar et al., 2009; Kosho et al., 2010; Malfait et al., 2010; Miyake et al., 2010]. Eight families were of Japanese origin, three of Turkish origin, one of Austrian origin, and one of Indian origin. The median patients' age at their initial publication was 4 years and 1 month (range, 0 day–32 years): 7 months (range, 0 day–6 years) in ATCS, 12.5 years in EDSKT (range, 2 years–32 years), and 21 years (range, 12 years–22 years) in MCEDS.

CHST14 mutations included V49X in two families (ATCS, MCEDS), K69X in one (EDSKT), R135G in one (ATCS), L137Q in one (ATCS), F209S in one (EDSKT), R213P in one (ATCS), P281L in eight (EDSKT), C289S in one (EDSKT), Y293C in four (one ATCS, three EDSKT), and E334GfsX107 in one (MCEDS). Sulfotransferase activity of COS-7 cells transfected with *CHST14* containing K69X, P281L, C289S, or Y293C mutation was decreased at almost the same level, suggesting that loss-of-function mutations in *CHST14*, that is to say D4ST1 deficiency, would cause these disorders [Miyake et al., 2010].

Characteristic craniofacial features at birth to early infancy (large fontanelle, hypertelorism, short and downslanting palpebral fissures, blue sclerae, short nose with hypoplastic columella, low-set and rotated ears, high palate, long philtrum, thin upper lip vermilion, small mouth, and micro-retrognathia) were noted in most patients with ATCS, EDSKT, and MCEDS. Slender and asymmetrical facial shapes with protruding jaws from school age, commonly observed in patients with EDSKT, were also described in ATCS2 at age 15 years, ATCS3 at age 6 years, ATCS7 at age 8 years [Dündar et al., 2009], and in MCEDS1 at age 21 years [Malfait et al., 2010]. A pair of ATCS siblings had palatal defects: ATCS4 with cleft lip and palate, which was surgically repaired, and ATCS5 with cleft soft palate [Sonoda and Kouno, 2000].

Congenital multiple contractures, most specifically adduction–flexion contractures of thumbs and talipes equinovarus,

TABLE I. Clinical Characteristics of Reported Patients With D4ST1 Deficiency (Continued)

Family	Patient	Origin	*CHST14* Mutations	Age at initial publication (d, days; m, months; y, years)	Sex	Craniofacial															Skeletal										Cutaneous						Cardiovascular				Gastrointestinal		
						Large fontanelle (early childhood)	Hypertelorism	Down-slanting palpebral fissures	Blue sclerae	Short nose with hypoplastic columella	Ear deformities	Palatal abnormalities	Long philtrum and thin upper lip	Small mouth/micro-retrognathia in infancy	Short neck	Slender face/protruding jaw from school age	Facial asymmetricity from school age	Malformed habitus/slender build	Congenital multiple contractions	Recurrent/chronic joint dislocations	Pectus deformities	Spinal deformities	Peculiar fingers (tapering, slender and cylindrical)	Progressive talipes deformities	Hyperextensibility/redundancy	Bruisability	Fragility/atrophic scars	Fine/Arrogeria-like palmar creases	Hyperalgesia to pressure	Recurrent subcutaneous infections/fistula	Congenital heart defects	Valve abnormalities	Large subcutaneous hematomas	(Henoch-Schönlein) purpura	Constipation	Others
ATCS																																										
1	1	Turkish	V49X homo	3.5y	F	+	+	+	+		P, PR	H	+		+				+				+																			
	2			1.5y	M	+	+	+	+	+	P, PR		+		+	+a		+a	+	+a	Exa	KSa	+	Planus, valgus#				+a				–									
	3			6y	F		+	+		+	P		+			+	+	+	+		F–T	S	+	Varus				+													
2	4	Japanese	Y293C homo	4y	M	+	+	+		+	LS	CL/CP	+						+	+	Ca		+	Planus, valgus																	
	5			7m	M	+	+	+		+	LS	CSP	+						+	+			+									ASD									
3	6	Austrian	R213P homo	0d†	M	+	+	+			PR, LS				+				+			S	+									ASD, CoA								Common mesentery
	7			12m	M	+	+	+	+		D, PR				+	+a		+a	+		F–Ta		+	Planus, valgus#				+a				–								Absence of gastrocolic omentum, spontaneous volvulus of small intestine
4	8	Turkish	R135G / L137Q	1–4m†	F														+																					
	9			1–4m†	M														+																					
	10			1–4m†	M														+																					
	11			3m	M	+	+	+	+		D, LS	H	+		+				+				+									–									
MCEDS																																										
1	1	Turkish	V49X homo	22y	F	+			+		+	PR, LS	H	+			+	+	+	+		F–T	KS	+	Planus, valgus	+	+	+	+		+	–	–							Hiatal hernia, gastroesphageal reflux, abdominal pain
	2			21y	F	+			+	+			H	+						+	+	F–T	S	+	Small, broad	+	+	+	+											
2	3	Indian	E334GfsX107 homo	12y	F					+		LS		–					+	+	+		KS	+	Planus, valgus	+	+	+	+		+									Duodenum obstruction due to malrotation
EDSKT																																										
1	1	Japanese	P281L / Y293C	11y	F	+	+	+	+	+	LS	H	+	+		+	+	+	+	+	Ex	KS	+	Planus, valgus	+	+	+	+	+	+	ASD	TR, TVP, MVP	+	–	+	Gastric ulcer§			
2	2	Japanese	P281L homo	14y	F	+	+	+	+	+	LS	H	+	+		+	+	+	+	+	F–T	S	+	Cavus, valgus	+	+	+	+	+	+	–		+	+§	+	Diverticular perforation§			
3	3	Japanese	P281L homo	32y	M	+	+	+	+	+	LS	H	+	+		+	+	+	+	+	F–T	KS	+	Planus, valgus	+	+	+	+	+	+		AR, ARD, MR	+	+	+	Diverticular perforation			
4	4	Japanese	K69X / P281L	32y	M		+		+			H				+	+	+	+		Ex	KS	+	Planus, valgus	+	+	–	+	–	–			+	+	–				
5	5	Japanese	P281L / C289S	20y	F	+	+	+	+	+	LS	H	+	+		+	+	+	+	+	Ex	S	+	Planus, valgus	+	+	+	+	+	+		AR, MR, IE	+	–	+				
6	6	Japanese	P281L / Y293C	4y	F	+	+	+	+	+	LS	H	+						+	+	Ex	S	+	Planus	+	+	+	+	+	+			+	–	+				
Present report (EDSKT)																																										
7	7	Japanese	P281L / Y293C	2y	M	+	+	+	+	+	PR, LS	H	+	+					+	+	F–T	S	+	Planus, valgus	+	+	+	+	–	+	–	ARD	–	–	+				
8	8	Japanese	F209S / P281L	6y	M	+	+	+	+	+	PR, LS	H	+	+					+	+	Ex		+	Planus	+	+	–	+	+	–	PDA	MVP	+	–	+	Abdominal pain			

ATCS, adducted thumb-clubfoot syndrome; EDSKT, Ehlers–Danlos Syndrome, Kosho Type; MCEDS, Musculocontractural Ehlers–Danlos Syndrome
+, present; Blank, information not available; †, died; F, female; M, male; P, prominent; PR, posteriorly rotated; LS, low set; D, dysplastic; H, high; CL, cleft lip; CP, cleft palate; CSP, cleft soft palate;
Ex, excavatum; F–T, flat and thin; Ca, carinatum; KS, kyphoscoliosis; S, scoliosis; ASD, atrial septal defect; CoA, coarctation of aorta; PDA, patent ductus arteriosus;
TR, tricuspid valve regurgitation; TVP, tricuspid valve prolapse; MVP, mitral valve prolapse; AR, aortic valve regurgitation; ARD, aortic root dilation; MR, mitral valve regurgitation; IE, infectious endocarditis
ATCS Patient 1 died at age 6 years [Dündar et al., 2009].
a, Information from reassessment by Dündar et al. [2009], describing ATCS P2 at age 15 years and ATCS P7 at age 8 years
b, Information from reassessment by Kosho et al. [2016], describing EDSKT1 at age 16 years and EDSKT2 at age 32 years

TABLE II. Clinical Characteristics of Reported Patients With D4ST1 Deficiency

		Urogenital			Ophthalmological						Development			Growth (prenatal)				Growth (postnatal)				
Family	Patient	Nephro (Cysto) lithiasis	Cryptorchidism	Others	Breast development	Strabismus	Refractive errors	Glaucoma/elevated intraocular pressure	Others	Hearing impairment	Ventricular abnormalities (brain)	Gross motor delay	Age of unassisted walk (y, years; m, months)	Mental delay	Gestational weeks	Birth length (centile or SD)	Birth weight (centile or SD)	Birth OFC (centile or SD)	Age (y, years; m, months)	Height (centile or SD)	Weight (centile or SD)	OFC (centile or SD)	References
ATCS																							
1	1					+					Enl	+	No	+	Term				3.5y	25-50th	50th	50th	Dündar et al., 1997
	2					+		+			Asym	+		+c	Term				1.5y	50th	10th	10–25th	Dündar et al., 1997
																			15ya	25–50th	<3rd		Dündar et al., 2009
	3					+													6y	10–25th	<3rd		Dündar et al., 2009
2	4		+	Hydronephrosis										–	39wk	–0.6	–0.9	–0.8	4y2m	–3.9	–1.8	–0.9	Sonoda and Kouno, 2000
	5		+	Hydronephrosis, inguinal hernia								–		–	38wk	–1.6	–1.3	–0.5	7m	–2.1	–1.4	–1.1	Sonoda and Kouno, 2000
3	6		+	Horseshoe kidney							Enl				32wk	25th	10th	25th					Janecke et al., 2001
	7		+			+					Asym	–		–	38wk	50th	25th	50th	8ya	10-25th	<3rd		Janecke et al., 2001
																							Dündar et al., 2009
4	8																						Dündar et al., 2001
	9																						Dündar et al., 2001
	10																						Dündar et al., 2001
	11	+	+	Inguinal hernia							Enl, Asym								3m	<3rd	3–10th	10th	Dündar et al., 2001
MCEDS																							
1	1	+			–		My	+	Retinal detachment, pthysis bulbi	+		+	4y		42wk	±0	–0.67		22y	–2.0		±0	Malfait et al., 2010
	2	+		Hydronephrosis, renal ptosis, ureteral stenosis	–		My	+	Retinal detachment	+		+	2y		42wk				14y	+0.68		>2.0	
2	3						My		Microcornea			+			Term		–0.88						Malfait et al., 2010
EDSKT																							
1	1			Bladder dilation, recurrent UTI, involuntary contractionb	–b	+	Hy	–	Microcornea	+	Enl	+	2y	+d	42wk	0.1	–1.3	–1.0	7y	+0.8	–1.0	±0	Kosho et al., 2005
																			11y	+0.2	–2	+0.2	Kosho et al., 2010
																			16y	+0.3	–0.4	+0.2	
2	2	+		Atonic bladder, recurrent UTI	–b	+	My, As	+b		+		+	No	–	Term		–2.0		15y	–3.2			Kosho et al., 2005
																							Kosho et al., 2010
3	3		+	Hypogonadism		+	My, As	–	Microphthalmia	+		+		–	40wk	+1.3	+0.5	+0.8	30y	+1.2	–1.7		Kosho et al., 2010
4	4					–	–	–	Retinal detachment	–				+					23y	–0.4	–2.4		Yasui et al., 2003
																							Kosho et al., 2010
5	5	+		Delayed menarche, irregular menstruation	–	+	My, As	+		–		+	2y2m	–	39wk	–1.1	–0.4	+1.0	19y	–0.1	–0.8		Kosho et al., 2010
6	6					+	My, As	+		+		+	1y5m	–	41wk	–1.2	–0.5	–0.6	4y	–1.2	–1.3	–0.9	Kosho et al., 2010
Present report																							
7	7		+			+	Hy, As, Am	–				+	No	+	38wk3d	–1.3	+0.2	+0.4	2y	–2.2	–2.4	–1.2	Patient 1
8	8		+			+				–	Enl	+	2y6m	–	38wk	+0.3	+0.3	–0.5	6y	–0.7	–1.4	+0.1	Patient 2

ATCS, adducted thumb-clubfoot syndrome; EDSKT, Ehlers-Danlos Syndrome, Kosho Type; MCEDS, Musculocontractural Ehlers-Danlos Syndome
+, present; Blank, information not available; UTI, urinary tract infection; Hy, hyperopia; My, myopia; As, astigmatism; Am, amblyopia; Enl, enlargement; Asym, asymmetry; No, not ambulant
a, Information from reassessment by Dündar et al. [2009], describing ATCS P2 at age 15 years and AFCS P7 at age 8 years
b, Information from reassessment by Kosho et al. [2010], describing EDSKT1 at age 16 years and EDSKT at age 32 years
c, IQ was 91 at Porteus test and 86 at Goodenough test at age 7 years and 2 months [Janecke et al., 2001];
d, mild learning dissability

were cardinal features in patients with ATCS, EDSKT, and MCEDS. Peculiar fingers described as "tapering," "slender," and "cylindrical" were also common features. Aberrant finger movement was described in EDSKT1 [Kosho et al., 2010], EDSKT7, and EDSKT8. EDSKT1, EDSKT2, EDSKT3, and EDSKT5 were found to have tendon abnormalities such as anomalous insertions of flexor muscles, which might result in contractures [Kosho et al., 2005, 2010]. In childhood, spinal deformities (scoliosis, kyphoscoliosis) and talipes deformities (planus, valgus) occurred and progressed. Malfanoid habitus, recurrent joint dislocations, and pectus deformities (flat and thin, excavatum, carinatum) were also evident. Talipes equinovarus in seven EDSKT patients and MCEDS3 was surgically repaired [Kosho et al., 2005, 2010; Malfait et al., 2010]. EDSKT3 received tendon transplantations for defects of tendons to bilateral thumbs, and EDSKT4 received surgical fixation of bilateral ankle joints as well as surgery for carpal tunnel syndrome [Kosho et al., 2010]. MCEDS1 underwent surgery for rapidly worsened kyphoscoliosis at age 14 years [Malfait et al., 2010].

Bone mineral density (BMD) was decreased in ATCS2 at age 15 years (Z score −1.6), ATCS3 at age 6 years (Z score −4.6) [Dündar et al., 2009], EDSKT2 at age 29 years (Z score −2.4 for the lumbar spine 1–4, −2.3 for the 33% radius), and EDSKT3 at age 31 years (Z score −3.7 for the lumbar spine 1–4, −3.6 for the femoral neck) [unpublished data], whereas BMD was normal in ATCS7 at age 8 years [Dündar et al., 2009] and EDSKT1 at age 15 years (Z score +1.6 for the lumbar spine 1–4, −0.9 for the femoral neck) [unpublished data]. Urine N-telopeptide of collagen type I (NTX), an osteoclast marker, was increased at 92.8 nmol BCE/mmol Cr in EDSKT1 at age 16 years, 70.3 nmol BCE/mmol Cr in EDSKT2 at age 28 years, and 238.4 nmol BCE/mmol Cr in EDSKT3 at age 31 years [unpublished data] (normal values for premenopausal females, 9.3–54.3; males, 13.0–66.2), whereas serum bone specific alkaline phosphatase (BAP), an osteoblast marker, was normal at 12.5 U/L in EDSKT1 at age 16 years, 25.6 U/L in EDSKT2 at age 28 years, and 15.1 U/L in EDSKT3 at age 31 years (normal values, 9.6–35.4) [unpublished data]. These results in biochemical markers of bone turnover suggested an increase in osteoclast activity with normal osteoblast activity, which could cause oeteopenia or osteoporosis.

Radiologically, diaphysial narrowing of phalanges and metacarpals was noted in EDSKT1 at age 11 and 16 years, EDSKT2 at age 10 and 28 years, EDSKT3 at age 31 years, EDSKT5 at age 19 years [Kosho et al., 2005, 2010], and EDSKT7 at age 2 years and 6 months. Talipes valgus and planus or cavum, with diaphysial narrowing of phalanges and metatarsals, were noted in ATCS7 at age 8 years [Dündar et al., 2009], EDSKT1 at age 11 and 16 years, EDSKT2 at age 14 and 28 years, EDSKT6 at age 4 years [Kosho et al., 2005, 2010], and EDSKT7 at age 2 years and 6 months. Tall vertebral bodies were noted in EDSKT1 at age 11 and 16 years, EDSKT2 at age 14 and 28 years, EDSKT3 at age 31 years, EDSKT4 at age 31 years, EDSKT5 at age 19 years [Kosho et al., 2005, 2010], and MCEDS2 at age 21 years [Malfait et al., 2010], whereas they were not noted in EDSKT6 at age 2 years [Kosho et al., 2010] and EDSKT7 at age 2 years and 6 months.

Cutaneous features were common in most patients with EDSKT and MCEDS, including hyperextensibility to redundancy, bruisability, fragility leading to atrophic scars, acrogeria-like fine palmar creases or wrinkles, hyperalgesia to pressure, and recurrent subcutaneous infections with fistula formation, which lead to skin defects including decubitus necessitating plastic surgery in EDSKT2 [Kosho et al., 2005, 2010]. Excessive palmar creases were observed in ATCS2, ATCS3, and ATCS7, and delayed wound healing and ecchymoses were also recorded ATCS patients [Dündar et al., 2009]. Palmar creases increased and became deeper according to the ages, as compared among photographs of EDSKT1 at age 11 and 16 years, EDSKT2 at age 5 years and 32 years, EDSKT3 at age 32 years, EDSKT5 at age 19years, and EDSKT6 at age 4 years [Kosho et al., 2005, 2010].

Seven patients with EDSKT suffered from large subcutaneous hematomas, which sometimes progressed acutely and massively to be treated intensively (admission, blood transfusion, surgical drainage). These lesions were supposed to be caused by rupture of subcutaneous arteries or veins. Hematoma formation was mentioned in a follow-up observation of ATCS patients [Dündar et al., 2009]. Bleeding time was prolonged in ATCS7 (9 min) [Dündar et al., 2009] and EDSKT4 (11 min) [Yasui et al., 2003; Kosho et al., 2010], whereas it was normal in EDSKT1 (3 min) [Kosho et al., 2005], EDSKT3 (1 min) [unpublished data], and EDSKT7 (1.3 min). EDSKT1 had, to prevent large subcutaneous hematomas, intranasal administration of 1-desamino-8-D-arginine vasopressin (DDAVP) after injuries [Kosho et al., 2005, 2010]. A large hematoma over the buttocks in EDSKT4 was treated with intranasal DDAVP and intramuscular conjugated estrogen [Yasui et al., 2003; Kosho et al., 2010].

Two ATCS and two EDSKT patients had congenital heart defects (atrial septal defect was the most common, observed in three), and five EDSKT patients had cardiac valve abnormalities. EDSKT5 suffered from infectious endocarditis probably resulting from aortic valve or mitral valve regurgitation, and underwent surgery. Three adult patients with EDSKT developed pneumothorax or hemopneumothorax, treated with chest tube drainage; and two of them suffered from diverticular perforation, treated surgically. Various gastrointestinal abnormalities were observed: Constipation in seven EDSKT patients and abdominal pain in one EDSKT and one MCEDS patients, as well as common mesentery in ATCS6, absent gastrocolic omentum and spontaneous volvulus of small intestine in ATCS7, gastric ulcer necessitating partial gastrectomy in EDSKT1, and duodenum obstruction due to malrotation treated surgically in MCEDS3 [Janecke et al., 2001; Dündar et al., 2009; Kosho et al., 2010; Malfait et al., 2010].

Urological complications included nephrolithiasis or cystolithiasis in one ATCS, two EDSKT, and two MCEDS patients; hydronephrosis in two ATCS and one MCEDS patients, dilated or atonic bladder with recurrent urinary tract infection in two EDSKT patients, and horseshoe kidney in one ATCS patient. Hydronephrosis in MCEDS2 was caused by renal ptosis and ureteral stenosis, for which a ureteral stent was placed with a laparoscopic procedure, complicated by severe hemorrhage due to excessive tissue fragility [Malfait et al., 2010].

Cryptorchidism was observed in five ATCS and three EDSKT male patients. EDSKT3, who received orchiopexy, showed hypogonadism in adulthood. In female patients older than adolescence, poor breast development was noted in three EDSKT (EDSKT1 and

EDSKT2 showed normal menstruation cycles; EDSKT5 showed delayed menarche and irregular menstruation cycles) and two MCEDS patients. No female patients have been reported to be pregnant.

Various ophthalmological complications were observed: Strabismus in four ATCS and seven EDSKT patients, refractive errors in six EDSKT and three MCEDS patients, glaucoma or elevated intraocular pressure in one ATCS, three EDSKT, and two MCEDS patients; microcornea or microphthalmia in two EDSKT and one MCEDS patients, and retinal detachment in one EDSKT and two MCEDS. Retinal detachment in EDSKT4 [Kosho et al., 2010] and glaucoma in MCEDS1 [Malfait et al., 2010] required surgery. Hearing impairment was noted in four EDSKT patients (predominantly for high-pitched sound in EDSKT1, EDSKT2, and EDSKT6) and two MCEDS.

Gross motor developmental delay was observed in two ATCS, seven EDSKT, and three MCEDS patients; and ages of unassisted walk in patients who accomplished it ranged from 1 year and 5 months to 4 years (median, 2 years and 1 month). EDSKT2, at age 32 years, could not walk unassisted because of severe foot deformities and muscle weakness of the legs [Kosho et al., 2010]. An underlying myopathic process was suggested in ATCS2 because of reduced amplitude muscle action potentials with normal distal latency time and nerve conduction velocity, whereas muscle biopsy did not reveal any histological abnormality [Dündar et al., 1997]. Mild mental delay was suggested in two ATCS and two EDSKT patients. ATCS2 was reported to have global psychomotor delay at the initial publication [Dündar et al., 1997], whereas his IQ was around 90 at age 7 years and 2 months [Janecke et al., 2001]. Five ATCS and two EDSKT patients showed ventricular enlargement and/or asymmetry on brain ultrasonography, CT or MRI. ATCS7 also showed absence of the left septum pellucidum [Janecke et al., 2001]. EDSKT6 had tethering of a spinal cord, and underwent duraplasty [Kosho et al., 2010].

Growth assessment was performed using data described with SD scores, excluding data described with centile scores. Patients with *CHST14* mutations showed mild prenatal growth retardation: The mean birth length −0.5 SD and the median −0.6 SD (n = 9; range, −1.6 SD to +1.3 SD); the mean birth weight −0.6 SD and the median −0.67 SD (n = 11; range, −2.0 SD to +0.5 SD); and the mean birth OFC −0.2 SD and the median −0.5 SD (n = 8; range, −1.0 SD to +1.0 SD). Postnatal growth was also mildly impaired with slenderness and relative macrocephaly: The mean height −0.9 SD and the median −0.6 SD (14 data from 12 patients; range, −3.9 SD to +1.2 SD); the mean weight −1.5 SD and the median −1.4 SD (11 data from 9 patients; range, −2.4 SD to −0.4 SD); the mean OFC −0.2 SD and the median ±0 SD (10 data from 8 patients; range, −1.2 SD to >2.0 SD).

Light microscopic investigations on skin specimens from EDSKT5 and EDSKT6 showed that fine collagen fibers were predominant in the reticular to papillary dermis and normally thick collagen bundles were markedly reduced [Miyake et al., 2010]. Electron microscopic investigations of the specimens showed that collagen fibrils were dispersed in the reticular dermis, compared with regularly and tightly assembled ones observed in the control, whereas each collagen fibril was smooth and round, not varying in size and shape, similar to each fibril of the control [Miyake et al., 2010]. These findings suggested that the main pathological basis of this disorder would be insufficient assembly of collagen fibrils, compatible with the evidence that dermatan sulfate of decorin proteoglycan, a key regulator of collagen fibril assembly that contains both chondroitin sulfate and dermatan sulfate in its glycosaminoglycan chains and controls the distance between collagen fibrils, was found to be completely lost and replaced by chondroitin sulfate in patients' fibroblasts [Miyake et al., 2010]. However, both light microscopic and electron microscopic findings of skin were assessed as normal in ATCS7 [Dündar et al., 2009]. In MCEDS2, most collagen bundles were small-sized, some of which were composed of variable diameter collagen fibrils separated by irregular interfibrillar spaces [Malfait et al., 2010].

This comprehensive review of the patients with loss-of-function mutations in *CHST14* (D4ST1 deficiency) supports the notion that ATCS, EDSKT, and MCEDS would be a single clinical entity with variable inter- and intra-familial expressions and with different presentations depending on the patients' ages at diagnosis or at publication. The disorder, we preferably would like to coin simply as EDS due to D4ST1 deficiency or D4ST1 deficient EDS (DD-EDS), is a clinically recognizable syndrome, characterized by progressive multisystem fragility-related manifestations including joint dislocations and deformities, skin hyperextensibility, bruisability, and fragility; recurrent large subcutaneous hematomas, and other cardiac valvular, respiratory, gastrointestinal, and ocular complications, which are considered to result from connective tissue weakness and be consequences of insufficient decorin-mediated assembly of collagen fibrils caused by D4ST1 deficiency. The disorder also shows various malformations including distinct craniofacial features, multiple congenital contractures, and congenital defects in cardiovascular, gastrointestinal, renal, ocular, and central nervous systems, which might not simply be accountable for connective tissue weakness but could be considered as inborn errors of development. In a recent review focusing on ATCS, Zhang et al. [2010] state that D4ST1 deficiency is the only recognized condition resulting from a defect specific to DS biosynthesis, and that the disorder emphasizes the roles D4ST1 play in human development and extracellular matrix maintenance.

DD-EDS could be detected at birth from characteristic craniofacial and skeletal features and molecular genetic testing gives definitive diagnosis. Initial screening for congenital cardiac, ocular, and renal abnormalities and hearing loss would be necessary. In infancy, orthopedic intervention for talipes equinovarus (serial plaster casts, surgery) as well as physical therapy for motor developmental delay would be the center of management. Laxatives and/or enema are considered in patients with constipation. Surgical fixation is considered for cryptorchidism in males. Regular follow-up for ophthalmological (strabismus, refractive errors, glaucoma), otological (otitis media with effusion, hearing loss), urological (urination, bladder enlargement), and cardiovascular (valve abnormalities, aortic root dilation) problems should be continued. After walking independently, attention should be paid to progressive foot deformities and trauma that could cause skin lacerations, joint dislocations, and massive subcutaneous hematomas. Intranasal DDAVP after injuries is considered to prevent large subcutaneous hematomas. From adolescence, assessment of spinal deformities (scoliosis, kyphoscoliosis) and secondary sex

characteristics (breast development in females and gonadal function in males) would be necessary. In adulthood, appropriate treatments should be performed on occasional emergency complications ([hemo]peumothorax, diverticular perforation). Wrist-type sphygmomanometer would be suitable for patients with hyperalgesia to pressure [unpublished observation].

Very recently, Janecke et al. [2011] have claimed that it would lead to confusion for clinicians and researchers to categorize the D4ST1 deficiency into a type of EDS and that an appropriate term should be "Dermatan sulfate-deficient adducted thumb-clubfoot syndrome." The reasons were described as follows: Clinically, "adducted thumb" and "clubfoot" would be the most distinguishable features at birth; etiologically, the molecular basis would differ substantially from EDS. In reply to the article, we have presented sufficient evidences for categorizing the disorder into a type of EDS: Clinically, the disorder would satisfy all the hallmarks of EDS (skin hyperextensibility, joint hypermobility, and tissue fragility affecting the skin, ligaments, joints, blood vessels, and internal organs), and the patients should be treated as having generalized connective tissue fragility in the lifelong management; etiologically, multisystem fragility in the disorder was found to be caused by impaired assembly of collagen fibrils caused by dermatan sulfate loss in the decorin glycosaminoglycan chain [Kosho et al., submitted].

In conclusion, ATCS, EDSKT, and MCEDS; which were found independently to be caused by D4ST1 deficiency, would be a single clinical entity with variable expressions and with different presentations depending on the patients' ages. The syndrome is characterized by a unique set of clinical features including progressive multisystem fragility-related manifestations (joint dislocations and deformities, skin hyperextensibility, bruisability, and fragility; recurrent large subcutaneous hematomas, and other cardiac valvular, respiratory, gastrointestinal, and ocular complications) resulting from impaired assembly of collagen fibrils, as well as various malformations (craniofacial features, multiple congenital contractures, and congenital defects in cardiovascular, gastrointestinal, renal, ocular, and central nervous systems) resulting from inborn errors of development.

ACKNOWLEDGMENTS

The authors express their gratitude to the patients and their families for participating in this study. They are also thankful to Dr. Inaba (Department of Pediatrics, Shinshu University School of Medicine) for his comments on a neurological assessment and Miss Kunimi for her technical assistance. This work was mainly supported by Research on Intractable Diseases from Japanese Ministry of Health, Welfare, and Labor (#2141039040) (N.O., N. Miyake, Y.F., N. Matsumoto, T.K.).

REFERENCES

Cheng S, Maeda T, Yamagata Z, Tomiwa K, Yamakawa N. Japan Children's Study Group. 2010. Comparison of factors contributing to developmental attainment of children between 9 and 18 months. J Epidemiol 20:S452–S458.

Dündar M, Demiryilmaz F, Demiryilmaz I, Kumandas S, Erkilic K, Kendirch M, Tuncel M, Ozyazgan I, Tolmie JL. 1997. An autosomal recessive adducted thumb-club foot syndrome observed in Turkish cousins. Clin Genet 51:61–64.

Dündar M, Kurtoglu S, Elmas B, Demiryilmaz F, Candemir Z, Ozkul Y, Durak AC. 2001. A case with adducted thumb and club foot syndrome. Clin Dysmorphol 10:291–293.

Dündar M, Müller T, Zhang Q, Pan J, Steinmann B, Vodopiutz J, Gruber R, Sonoda T, Krabichler B, Utermann G, Baenziger JU, Zhang L, Janecke AR. 2009. Loss of dermatan-4-sulfotransferase 1 function results in adducted thumb-clubfoot syndrome. Am J Hum Genet 85:873–882.

Evers MR, Xia G, Kang HG, Schachner M, Baeziger JU. 2001. Molecular cloning and characterization of a dermatan-specific *N*-acetylgalactosamine 4-O-sulfotransferase. J Biol Chem 276:36344–36353.

Haga H, Yamada R, Ohnishi Y, Nakamura Y, Tanaka T. 2002. Gene-based SNP discovery as part of the Japanese Millennium Genome Project: Identification of 190,562 genetic variations in the human genome. J Hum Genet 47:605–610.

Janecke AR, Unsinn K, Kreczy A, Baldissera I, Gassner I, Neu N, Utermann G, Müller T. 2001. Adducted thumb-club foot syndrome in sibs of a consanguineous Austrian family. J Med Genet 38:265–269.

Janecke AR, Baenziger JU, Müller T, Dündar M. 2011. Letter to the Editors. Loss of dermatan-4-sulfotransferase 1 (D4ST1/*CHST14*) function represents the first dermatan sulfate biosynthesis defect, "Dermatan sulfate-deficient adducted thumb-clubfoot syndrome." Hum Mutat 32:484–485.

Kosho T, Takahashi J, Ohashi H, Nishimura G, Kato H, Fukushima Y. 2005. Ehlers-Danlos syndrome type VIB with characteristic facies, decreased curvatures of the spinal column, and joint contractures in two unrelated girls. Am J Med Genet Part A 138A:282–287.

Kosho T, Miyake N, Hatamochi A, Takahashi J, Kato H, Miyahara T, Igawa Y, Yasui H, Ishida T, Ono K, Kosuda T, Inoue A, Kohyama M, Hattori T, Ohashi H, Nishimura G, Kawamura R, Wakui K, Fukushima Y, Matsumoto N. 2010. A new Ehlers-Danlos syndrome with craniofacial characteristics, multiple congenital contractures, progressive joint and skin laxity, and multisystem fragility-related manifestations. Am J Med Genet Part A 152A:1333–1346.

Kosho T, Miyake N, Mizumoto S, Hatamochi A, Fukushima Y, Sugahara K, Matsumoto N. 2011. A response to: Loss of dermatan-4-sulfotransferase 1 (D4ST1/*CHST14*) function represents the first dermatan sulfate biosynthesis defect, "Dermatan sulfate-deficient adducted thumb-clubfoot syndrome". Which name is appropriate, "adducted thumb-clubfoot syndrome" or "Ehlers-Danlos syndrome"? (submitted).

Malfait F, Syx D, Vlummens P, Symoens S, Nampoothiri S, Hermanns-Lê Van Lear L, De Paepe A. 2010. Musculocontractural Ehlers-Danlos syndrome (former EDS type VIB) and adducted thumb clubfoot syndrome (ATCS) represent a single clinical entity caused by mutations in the dermatan-4-sulfotransferase 1 encoding *CHST14* gene. Hum Mutat 31:1233–1239.

Mikami T, Mizumoto S, Kago N, Kitagawa H, Sugahara K. 2003. Specificities of three distinct human chondroitin/dermatan N-acetylgalactosamine 4-O-sulfotransferases demonstrated using partially desulfated dermatan sulfate as an acceptor: Implication of differential roles in dermatan sulfate biosynthesis. J Biol Chem 278:36115–36127.

Miyake N, Kosho T, Mizumoto S, Furuichi T, Hatamochi A, Nagashima Y, Arai E, Takahashi K, Kawamura R, Wakui K, Takahashi J, Kato H, Yasui H, Ishida T, Ohashi H, Nishimura G, Shiina M, Saitsu H, Tsurusaki Y, Doi H, Fukushima Y, Ikegawa S, Yamada S, Sugahara K, Matsumoto N. 2010. Loss-of-function mutations of *CHST14* in a new type of Ehles-Danlos syndrome. Hum Mutat 31:966–974.

Sonoda T, Kouno K. 2000. Two brothers with distal arthrogryposis, peculiar facial appearance, cleft palate, short stature, hydronephrosis,

retentio testis, and normal intelligence: A new type of distal arthrogryposis? Am J Med Genet 91:280–285.

Trowbridge JM, Gallo RL. 2002. Dermatan sulfate: New functions from an old glycosaminoglycan. Glycobiol 12:117R–125R.

Yasui H, Adachi Y, Minami T, Ishida T, Kato Y, Imai K. 2003. Combination therapy of DDAVP and conjugated estrogens for a recurrent large subcutaneous hematoma in Ehlers-Danlos syndrome. Am J Hematol 72:71–72.

Zhang L, Müller T, Baenziger JU, Janecke AR. 2010. Congenital disorders of glycosylation with emphasis on loss of dermatan-4-sulfotransferase? Prog Mol Biol Transl Sci 93:289–307.

CLINICAL GENETICS An International Journal of Genetics, Molecular and Personalized Medicine

Clin Genet 2011: 80: 161–166
Printed in Singapore. All rights reserved

CLINICAL GENETICS
doi: 10.1111/j.1399-0004.2011.01721.x

Short Report

Exome sequencing of two patients in a family with atypical X-linked leukodystrophy

Tsurusaki Y, Okamoto N, Suzuki Y, Doi H, Saitsu H, Miyake N, Matsumoto N. Exome sequencing of two patients in a family with atypical X-linked leukodystrophy.
Clin Genet 2011: 80: 161–166. © John Wiley & Sons A/S, 2011

We encountered a family with two boys similarly showing brain atrophy with reduced white matter, hypoplasia of the brain stem and corpus callosum, spastic paralysis, and severe growth and mental retardation without speaking a word. The phenotype of these patients was not compatible with any known type of syndromic leukodystrophy. Presuming an X-linked disorder, we performed next-generation sequencing (NGS) of the transcripts of the entire X chromosome. A single lane of exome NGS in each patient was sufficient. Six potential mutations were found in both affected boys. Two missense mutations, including c.92T>C (p.V31A) in *L1CAM*, were potentially pathogenic, but this remained inconclusive. The other four could be excluded. Because the patients did not show adducted thumbs or hydrocephalus, the *L1CAM* change in this family can be interpreted as different scenarios. Personal genome analysis using NGS is certainly powerful, but interpretation of the data can be a substantial challenge requiring a lot of tasks.

Conflict of interest

None of the authors have any conflicts of interest to disclose.

Y Tsurusaki[a], N Okamoto[b], Y Suzuki[c], H Doi[a], H Saitsu[a], N Miyake[a] and N Matsumoto[a]

[a]Department of Human Genetics, Yokohama City University Graduate School of Medicine, Kanazawa-ku, Yokohama, Japan, and [b]Department of Medical Genetics, and [c]Department of Pediatric Neurology, Osaka Medical Center and Research Institute for Maternal and Child Health, Murodo-cho, Izumi, Japan

Key words: atypical phenotype – exome sequencing – *L1CAM* – X-linked leukodystrophy

Corresponding author: Naomichi Matsumoto, Department of Human Genetics, Yokohama City University Graduate School of Medicine, 3-9 Fukuura, Kanazawa-ku, Yokohama 236-0004, Japan.
Tel.: +81-45-787-2606;
fax: +81-45-786-5219;
e-mail: naomat@yokohama-cu.ac.jp

Received 4 May 2011, revised and accepted for publication 31 May 2011

Focused/selected gene and genomic characterization has usually been carried out in clinically homogeneous groups of multiple affected samples to make identification of genetic abnormalities more efficient. Microarrays and next-generation sequencing (NGS) have provided new avenues for human genetic research (1–6). Using such new technologies, researchers are able to analyze small numbers of patients on a genome-wide scale. Even very rare cases (such as when only a few compatible patients are available or atypical patients showing no similar phenotypes) can be realistic targets of genetic research, as the new technologies can identify aberrations in a single gene from within virtually the whole genome; this could not be achieved with conventional techniques.

We encountered a family with two affected males showing atypical leukodystrophy. The phenotype of these patients did not match any known type of syndromic leukodystrophy. Because we presumed that abnormality of an X-linked gene caused the atypical leukodystrophy in this family, we performed exome sequencing of most of the X-chromosome transcripts and identified an unexpected gene mutation in these patients.

Materials and methods

A family with atypical X-linked leukodystrophy

Two brothers, II-1 currently aged 19 years and II-2 currently aged 17 years, who have unrelated healthy parents, presented with similar clinical

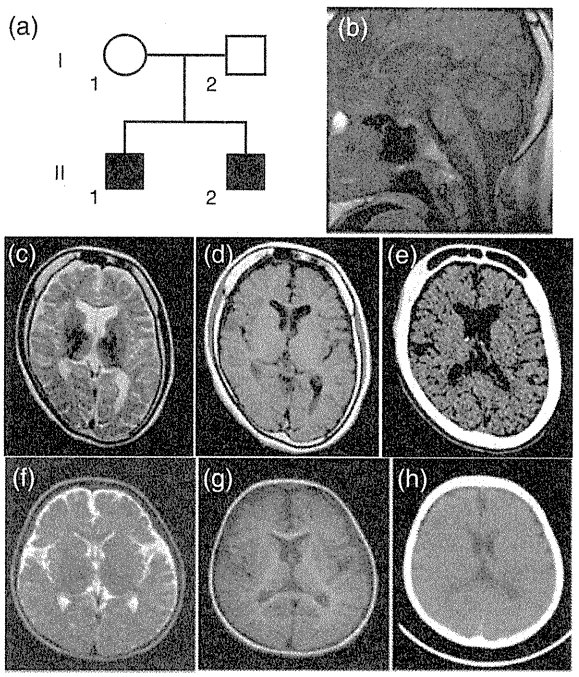

Fig. 1. Clinical features of the family. Familial pedigree (**a**). Brain magnetic resonance imaging (MRI) (**b**: T1-weighted image, **c**: T2-weighted image, **d**: T1-weighted image) of individual II-1 at 16 years old showing hypoplasia of the white matter, the brain stem and the corpus callosum. Brain computed tomographic (CT) images of individual II-1 at 19 years old (**e**) indicating a thick calvarium with enlarged frontal sinus as well as calcification of the choroid plexus in the atrophic brain. Brain MRI (**f**: T2-weighted image, **g**: T1-weighted image) of individual II-2 at 2 years old, also displaying hypoplasia of the white matter. Brain CT image of individual II-2 at 5 years old (**h**), also showing a thick calvarium.

features. Their mother did not show any neurological abnormalities (Fig. 1a).

Patient II-1

Patient II-1's birth weight was 2840 g at 40 weeks of gestational age. He had congenital nystagmus. He sat unsupported at 7 months old but after this his developmental milestones were delayed. He could creep at 18 months old. Spastic paralysis, especially in the lower extremities, became apparent. He was unable to stand unsupported. His mental development was severely delayed, and he needed special education from elementary school. He had suffered generalized epileptic seizures since he was 10 years old. He was confined to a wheelchair. He had severe mental retardation without speaking a word. His developmental quotient (DQ) at 9 years old was 19 by the Japanese standard method. Severe growth retardation [143 cm (<3%), 24 kg (<3%), occipitofrontal head circumference 49 cm (<3%) at 19 years] was also noted. He did not have dysmorphic features. Blood analysis revealed microcytic anemia [hemoglobin (Hb) 13.4 g/dl, mean corpuscular volume (MCV) (of red blood cell) 70.4 fl (normal: 89–99 fl), mean corpuscular hemoglobin (MCH) (of red blood cell) 23.1 pg (normal: 29–35 pg)] without any evidence of hemolysis or iron deficiency. Hormonal examination indicated that the levels of luteinizing hormone, follicle-stimulating hormone, and thyroid-stimulating hormone were all low [0.9 mIU/ml (normal: 1.2–8.0 mIU/ml), 2.5 mIU/ml (normal: 2.3–15.1 mIU/ml), <0.01 μIU/ml (normal: 0.5–5.0 μIU/ml), respectively]. He showed delayed puberty with small testes. Pubic hair only appeared at 17 years old. His bone age at 18 years old was 12.6 years (67%). Brain magnetic resonance imaging (MRI) at 16 years old revealed brain atrophy associated with reduced white matter and hypoplasia of the brain stem and the corpus callosum (Fig. 1b–d). No hydrocephalus or adducted thumb was observed. Brain computed tomography (CT) at 19 years old showed a thick calvarium with enlarged frontal sinus as well as calcification of the cerebellar tentorium and the choroid plexus (Fig. 1e).

Patient II-2

Patient II-2's birth weight was 2910 g at 37 weeks of gestational age. Developmental delay was apparent since he was 10 months old. Spastic paralysis (especially in the lower extremities), confinement to a wheelchair, severe mental retardation without speaking a word (DQ = 5 at 17 years old), and severe growth retardation [130 cm (<3%) and 27 kg (<3%) at 17 years] were phenotypes shared with his brother (II-1). Blood analysis revealed microcytic anemia (Hb 12.0 g/dl, MCV 61.1 fl, MCH 19.0 pg) without any evidence of hemolysis or iron deficiency. Hormonal examination indicated that the levels of luteinizing hormone, follicle-stimulating hormone, and thyroid-stimulating hormone were relatively low (1.9 mIU/ml, 4.2 mIU/ml, <0.23 μIU/ml, respectively). He also showed delayed puberty with small testes. Pubic hair appeared only at 17 years old. His bone age at 17 years old was 11 years (65%). Brain MRI at 2 years old revealed brain atrophy associated with reduced white matter and hypoplasia of the brain stem and corpus callosum (Fig. 1f,g). Brain CT at 5 years old showed a thick calvarium (Fig. 1h). No hydrocephalus or adducted thumb was observed. Most of the clinical features were similar to those of his brother except for the absence of nystagmus in patient II-2.

Genome-wide SNP genotyping

Genome-wide single-nucleotide polymorphism (SNP) genotyping was performed on individuals I-2, II-1, and II-2 using a GeneChip™ Human Mapping 10K Array Xba 142 2.0 (Affymetrix, Inc., Santa Clara, CA), according to the manufacturer's protocols. Mendelian error in the pedigree to exclude conflicted SNPs was checked using GCOS 1.2 (GeneChip Operating Software; Affymetrix) and batch analysis in GTYPE 4.0 (GeneChip Genotyping Analysis Software; Affymetrix), with the default setting for the mapping algorithm. The linked region, with SNP genotypes shared between individuals II-1 and II-2, was checked manually.

Genomic partitioning, short-read sequencing, and sequence alignment

Three micrograms of genomic DNA from the affected brothers (II-1 and II-2) was processed using a SureSelect X Chromosome test kit (1582 transcripts covering 3053 kb) (Agilent Technologies, Santa Clara, CA), according to the manufacturer's instructions. Captured DNAs were analyzed using an Illumina GAIIx (Illumina, Inc., San Diego, CA). We used only one of the eight lanes in the flow cell (Illumina) for paired-end, 76-bp reads per sample. Image analysis and base-calling were performed using sequence control software (SCS) real-time analysis and off-line BASECALLER software v1.8.0 (Illumina). Reads were aligned to the human reference genome (UCSC hg19, NCBI build 37.1) using the ELANDv2 algorithm in CASAVA_v1.7.0 (Illumina). The ELANDv2 algorithm can align 100-bp reads to a reference sequence and split the reads into multiple seeds.

Mapping strategy and variant annotation

Approximately 57.5 million reads from individual II-1 and 71.1 million reads from individual II-2 that passed the quality control (Path Filter) were mapped to the human reference genome using mapping and assembly with quality (MAQ) (7) (Fig. 2). MAQ was able to align 51 720 952 and 65 990 660 reads to the whole genome for individuals II-1 and II-2, respectively; these were then statistically analyzed for coverage using a script created by BITS Co., Ltd. (Tokyo, Japan). SNPs and insertions/deletions were extracted from the alignment data using an original script created by BITS Co., Ltd., along with information on the registered SNPs (dbSNP 131). A consensus quality score of 40 or more was used for the SNP analysis in MAQ. SNPs in MAQ-passed reads were annotated using the SeattleSeq website (http://gvs.gs.washington.edu/SeattleSeqAnnotation/). Variants found by each informatics method were selected in terms of location on chromosome X, unregistered variants (excluding registered SNPs), variants in known genes, variants in coding regions, variants excluding synonymous changes, and variants with an allele frequency of at least 90% (assuming a homozygous mutation). NEXTGENE software v2.0 (SoftGenetics, State College, PA) was also used to analyze the reads, with a default setting. Variants found by both of the informatics methods were selected. The variants found in common between individuals II-1 and II-2 were focused on, and confirmed as true positives by Sanger sequencing of polymerase chain reaction (PCR) products amplified from patient genomic DNA, except for variants within genes at segmental duplications. The pathological significance of the variants was evaluated using four different websites: POLYPHEN (Polymorphism Phenotyping; http://genetics.bwh.harvard.edu/pph/index.html), POLYPHEN-2 (http://genetics.bwh.harvard.edu/pph2/index.shtml), SIFT (http://sift.jcvi.org/) (output values less than 0.05 are deleterious), and MUTATIONTASTER (http://neurocore.charite.de/MutationTaster/).

Capillary sequencing

Possible pathological variants were confirmed by Sanger sequencing using an ABI 3500xl or ABI3100 autosequencer (Life Technologies, Carlsbad, CA), following the manufacturer's protocol. Sequencing data were analyzed using SEQUENCHER software (Gene Codes Corporation, Ann Arbor, MI).

Expression studies

The relative mRNA levels of *TMEM187* in cDNA of various fetal and adult human tissues (Human MTC™ Panel I and Human Fetal MTC™ Panel; Clontech, Mountain View, CA) were determined by quantitative real-time reverse transcription–polymerase chain reaction (RT-PCR) using TaqMan gene expression assays (Hs01920894_s1 for *TMEM187* and Hs00357333_g1 for β-actin as a control) (Life Technologies).

Results and discussion

Our coverage analysis indicated that for individuals II-1 and II-2, 79.2% and 78.8%, respectively, of the entire X-chromosome coding sequence (CDS) were completely covered, and 88.5% and 88.5%,

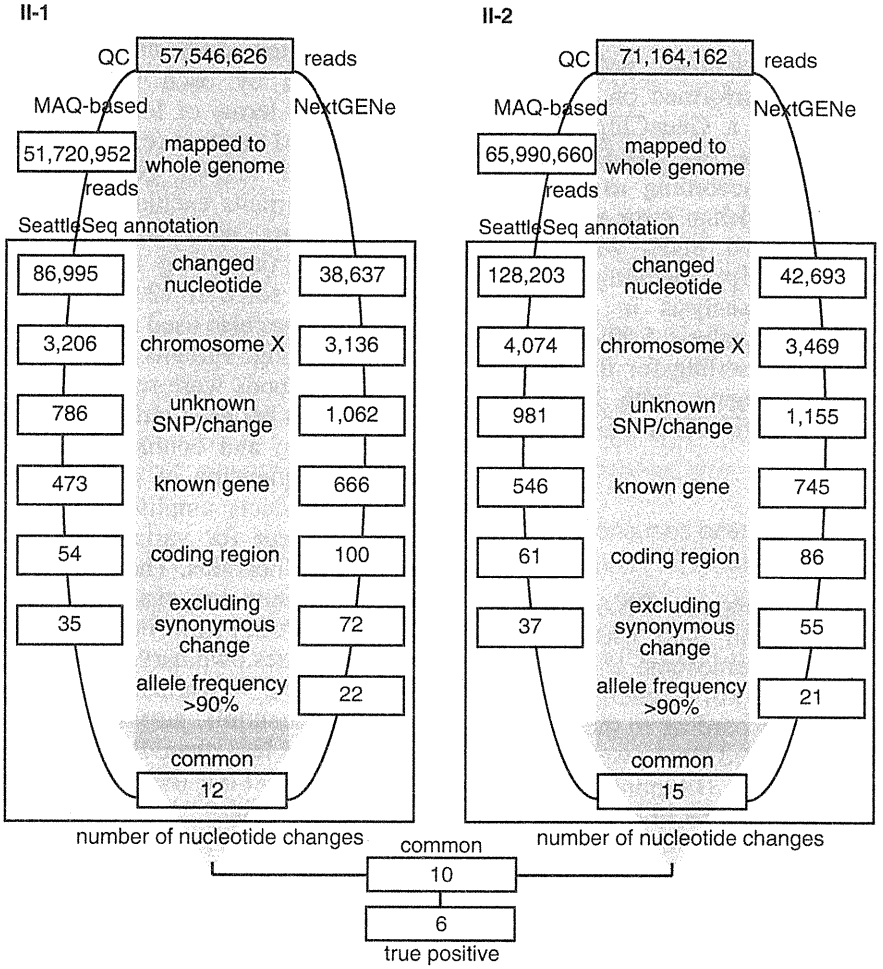

Fig. 2. Flow of informatics analysis. A MAQ-based method and NextGENe analysis were performed in individuals II-1 and II-2. The selection methods employed included variants compared with the human genome reference sequence, variants mapped to chromosome X, unknown variants [excluding registered single-nucleotide polymorphisms (SNPs)], variants in known genes, variants in coding regions, variants excluding synonymous changes, and variants common to the two informatics methods. Finally, the nucleotide changes in common between individuals II-1 and II-2 were focused on as potentially pathogenic mutations. True positive changes were confirmed by capillary sequencing of polymerase chain reaction (PCR) products amplified from genomic DNA.

respectively, of the CDS were at least 90% covered by reads. Using a single lane of sequencing per sample, the coverage with 20 reads or more comprised 89.6% and 89.7% of the CDS, and that with 100 reads or more comprised 87.6% and 89.7% of the CDS in individuals II-1 and II-2, respectively. SNP genotyping indicated that the region from rs727240 to rs721003 (UCSC genome browser hg19 assembly, chromosome X coordinates: 22131639–54454152; 32.2 Mb) was unlinked to the phenotype. Exome sequencing using two informatics methods successfully identified six potentially interesting changes as true positives in the linked region: *FAM123B* (RefSeq Gene ID NM_152424): c.85G>A (p.A29T), *FRMD7* (NM_194277): c.875T>C (p.L292P), *L1CAM* (NM_000425): c.92T>C (p.V31A), *TMEM187* (NM_003492): c.334G>A (p.A112T), *FLNA* (NM_001110556): c.1582G>A (p.V528M), and *LAGE3* (NM_006014): c.395G>A (p.R132Q).

The c.92T>C (p.V31A) variant in *L1CAM* was previously found in a patient with Hirschsprung disease, acrocallosal syndrome, and congenital hydrocephalus (8). *L1CAM* mutations cause a wide variety of clinical phenotypes: hydrocephalus due to stenosis of the aqueduct of Sylvius (MIM #307000), MASA syndrome (mental retardation, aphasia, shuffling gait, adducted thumb; MIM #303350), and X-linked agenesis of the corpus callosum (MIM #217990). Phenotypic variability, even within a family, has been noted, raising the caution that definite clinical diagnosis in single

Table 1. Characterization of nucleotide changes found by exome sequencing

	FAM123B	*FRMD7*	*L1CAM*	*TMEM187*	*FLNA*	*LAGE3*
Change	c.85G>A (p.A29T)	c.875T>C (p.L292P)	c.92T>C (p.V31A)	c.334G>A (p.A112T)	c.1582G>A (p.V528M)	c.395G>A (p.R132Q)
PolyPhen	Benign	Probably damaging	Benign	Benign	Possibly damaging	Benign
PolyPhen-2	Probably damaging	Probably damaging	Benign	Possibly damaging	Possibly damaging	Possibly damaging
SIFT	0.04	0.02	0.22	0.02	0.04	0.46
MutationTaster	Polymorphism	Disease causing	Disease causing	Polymorphism	Polymorphism	Polymorphism
Normal female	8/502[a]	2/502	2/502	1/502	15/502[a]	4/502
Normal male	1/118	0/117	0/118	0/118		1/86
Note		No nystagmus in II-2				

[a]Including one homozygous female. Underlining means that this result excludes the variant as potentially causative. Grayed shading indicates the variants that could not be excluded; between these two, the *L1CAM* variant is more likely to be causative.

cases is often impossible (9). Phenotypic features compatible with the *L1CAM* mutation in our patients include spastic paralysis, aphasia, severe mental and growth retardation, but atypical leukodystrophy and the absence of adducted thumbs were very rare or exceptional (9). A normal control study found that 2 of 251 normal females were heterozygous for this SNP, but none of 117 normal males carried the variant allele. One of the four web-based analyses of pathological significance (MutationTaster) indicated that this variant would be disease causing, while the others indicated that it would be benign (Table 1). X-linked hydrocephalus due to *L1CAM* mutations occurs in approximately 1/30 000 male births (10). Considering that the *L1CAM* mutation was found in 2/618 control alleles (0.32%), the change may be a rare polymorphism, a mutation causing lethality in the majority of affected males, or a mutation with low penetrance. Because we were unable to exclude this *L1CAM* change, its pathogenic status remains inconclusive.

We next examined c.85G>A in *FAM123B*, c.875T>C in *FRMD7*, c.1582G>A in *FLNA*, and c.395G>A in *LAGE3* in normal controls. The *FAM123B*, *FLNA*, and *LAGE3* variants were excluded as causative because a homozygous change was found in 1 of 251 female controls (*FAM123B* and *FLNA*) or a hemizygous change was found in 1 of 86 normal males (*LAGE3*). However, the thick calvarium in individuals II-1 and II-2 may be influenced by the *FAM123B* change, because it is causative for osteopathia striata with cranial sclerosis, an X-linked dominant disorder (MIM #300373) (11, 12). As the calvarium of the patients' mother having the heterozygous *FAM123B* change was not evaluated by CT, we could not confirm this possibility.

Only 2 of 251 control females carried the c.875T>C variant in *FRMD7* heterozygously, and none of 117 male controls carried this variant; thus, the pathogenicity of the *FMRD7* variant was inconclusive. Other *FRMD7* mutations cause X-linked congenital nystagmus 1 (MIM #310700) (13). However, the nystagmus found in individual II-1 was not observed in individual II-2, indicating that the variant in common between two brothers did not consistently cause nystagmus. Thus, it may not contribute to the phenotype in this family (Table 1).

We also evaluated the c.334G>A variant in *TMEM187*. Only 2 of 251 female controls carried this heterozygous change, and it was not found among 118 male controls. Two of the four programs (PolyPhen-2 and SIFT) indicated that it would be pathogenic. By Taqman assay, *TMEM187* was ubiquitously expressed in various fetal and adult tissues, including the brain (data not shown), leaving the effect of this mutation on the phenotype in these patients inconclusive (Table 1).

In conclusion, we found two possible but inconclusive variants in this family with two boys affected by atypical leukodystrophy. High-throughput technologies are clearly powerful to detect genomic changes, but evaluation of the data can be very difficult and should be performed cautiously. More knowledge of rare SNPs and mutations is absolutely necessary before any conclusions can be drawn.

Acknowledgements

We would like to thank the patients and their family members for their participation in this study. This work was supported by research grants from the Ministry of Health, Labour and Welfare

(to H. S., N. Miyake, and N. Matsumoto), the Japan Science and Technology Agency (to N. Matsumoto), a Grant-in-Aid for Scientific Research from the Japan Society for the Promotion of Science (to N. Matsumoto), and a Grant-in-Aid for Young Scientists from the Japan Society for the Promotion of Science (to H. D., N. Miyake, and H. S.).

References

1. Saitsu H, Kato M, Mizuguchi T et al. De novo mutations in the gene encoding STXBP1 (MUNC18-1) cause early infantile epileptic encephalopathy. Nat Genet 2008: 40: 782–788.
2. Check Hayden E. Genomics shifts focus to rare diseases. Nature 2009: 461: 458.
3. Biesecker LG. Exome sequencing makes medical genomics a reality. Nat Genet 2010: 42: 13–14.
4. Kuhlenbaumer G, Hullmann J, Appenzeller S. Novel genomic techniques open new avenues in the analysis of monogenic disorders. Hum Mutat 2011: 32: 144–151.
5. Miyake N, Kosho T, Mizumoto S et al. Loss-of-function mutations of CHST14 in a new type of Ehlers-Danlos syndrome. Hum Mutat 2010: 31: 966–974.
6. Ng SB, Bigham AW, Buckingham KJ et al. Exome sequencing identifies MLL2 mutations as a cause of Kabuki syndrome. Nat Genet 2010: 42: 790–793.
7. Li H, Ruan J, Durbin R. Mapping short DNA sequencing reads and calling variants using mapping quality scores. Genome Res 2008: 18: 1851–1858.
8. Nakakimura S, Sasaki F, Okada T et al. Hirschsprung's disease, acrocallosal syndrome, and congenital hydrocephalus: report of 2 patients and literature review. J Pediatr Surg 2008: 43: E13–E17.
9. Rietschel M, Friedl W, Uhlhaas S, Neugebauer M, Heimann D, Zerres K. MASA syndrome: clinical variability and linkage analysis. Am J Med Genet 1991: 41: 10–14.
10. Rosenthal A, Jouet M, Kenwrick S. Aberrant splicing of neural cell adhesion molecule L1 mRNA in a family with X-linked hydrocephalus. Nat Genet 1992: 2: 107–112.
11. Viot G, Lacombe D, David A et al. Osteopathia striata cranial sclerosis: non-random X-inactivation suggestive of X-linked dominant inheritance. Am J Med Genet 2002: 107: 1–4.
12. Jenkins ZA, van Kogelenberg M, Morgan T et al. Germline mutations in WTX cause a sclerosing skeletal dysplasia but do not predispose to tumorigenesis. Nat Genet 2009: 41: 95–100.
13. Tarpey P, Thomas S, Sarvananthan N et al. Mutations in FRMD7, a newly identified member of the FERM family, cause X-linked idiopathic congenital nystagmus. Nat Genet 2006: 38: 1242–1244.

RESEARCH ARTICLE

AMERICAN JOURNAL OF medical genetics PART A

Submicroscopic Deletion of 12q13 Including *HOXC* Gene Cluster With Skeletal Anomalies and Global Developmental Delay

Nobuhiko Okamoto,[1]* Daisuke Tamura,[2] Gen Nishimura,[3] Keiko Shimojima,[4] and Toshiyuki Yamamoto[4]

[1]Department of Medical Genetics, Osaka Medical Center and Research Institute for Maternal and Child Health, Osaka, Japan

[2]Department of Orthopedics, Osaka Medical Center and Research Institute for Maternal and Child Health, Osaka, Japan

[3]Department of Pediatric Imaging, Tokyo Metropolitan Children's Medical Center, Tokyo, Japan

[4]Tokyo Women's Medical University Institute for Integrated Medical Sciences, Tokyo, Japan

Received 13 May 2011; Accepted 4 September 2011

We report on a patient with a submicroscopic deletion of 12q13 detected by array-CGH and confirmed by FISH. He was haploinsufficient for the *HOXC* gene cluster and some other neighboring genes. *HOX* genes have an important role in the initial formation of the body. The patient showed characteristic features including severe kyphoscoliosis, digital abnormalities, cardiac anomaly, expressive language, and global developmental delay. Radiologic features of the fingers had some similarities with those for multiple synostosis syndrome. No human genetic disorders due to *HOXC* abnormalities are yet known. We tentatively assume that his skeletal anomalies are associated with haploinsufficiency of the *HOXC* gene cluster. Further studies are necessary to determine the clinical importance of haploinsufficiency of the *HOXC* gene cluster.

Key words: *HOX*; *HOXC*; array-CGH; kyphoscoliosis; multiple synostosis syndrome

How to Cite this Article:
Okamoto N, Tamura D, Nishimura G, Shimojima K, Yamamoto T. 2011. Submicroscopic deletion of 12q13 including *HOXC* gene cluster with skeletal anomalies and global developmental delay.
Am J Med Genet Part A 155:2997–3001.

INTRODUCTION

HOX genes have an important role in the initial formation of the body plan by providing positional information along the anterior–posterior body and limb axis and are associated with neural tube closure. *HOX* A, B, C, and D make a cluster on chromosomes 7, 17, 12, and 2, respectively. Each cluster consists of 9–11 genes from 13 paralogous groups. The order of the *HOX* genes along the chromosome correlates with their expression along the anterior/posterior axis of the embryo.

Some of the *HOX* genes are associated with genetic syndromes. Akarsu et al. [1996] reported that a polyalanine tract expansion in *HOXD13* causes synpolydactyly (OMIM #186000). Mortlock and Innis [1997] found a nonsense mutation in *HOXA13* among patients with hand-foot-genital syndrome (OMIM #140000). Thompson and Nguyen [2000] reported that megakaryocytic thrombocytopenia and radio-ulnar synostosis (OMIM #605432) are associated with *HOXA11* mutations. Shrimpton et al. [2004] reported a *HOXD10* mutation in a family with isolated congenital vertical talus and Charcot-Marie-Tooth disease (OMIM #142984). Tischfield et al. [2005] identified homozygous truncating mutations in *HOXA1* in patients with horizontal gaze abnormalities, deafness, facial weakness, hypoventilation, vascular malformations of the internal carotid arteries and cardiac outflow tract, intellectual disability, and autism spectrum disorder. Two syndromes associated with homozygous mutations of *HOXA1* are known as the Bosley-Salih-Alorainy syndrome and the Athabascan brainstem dysgenesis syndrome (OMIM #601536) [Bosley et al., 2008]. Alasti et al. [2008] reported a mutation in *HOXA2* in autosomal-recessive microtia (OMIM #612290).

Spitz et al. [2002] reported a t(2;8)(q31;p21) balanced translocation with breakpoints near the human *HOXD* complex. The patient had mesomelic dysplasia of the upper limbs and vertebral defects. Dlugaszewska et al. [2006] reported three patients with limb abnormalities and breakpoints involving chromosome 2q31. None of the three 2q31 breakpoints, which all mapped close to the *HOXD*

Additional supporting information may be found in the online version of this article.

Grant sponsor: Ministry of Health, Labour, and Welfare in Japan.

*Correspondence to:
Dr. Nobuhiko Okamoto, Department of Medical Genetics, Osaka Medical Center and Research Institute for Maternal and Child Health, 840 Murodo-cho, Izumi, Osaka 594-1101, Japan. E-mail: okamoto@osaka.email.ne.jp

Published online 8 November 2011 in Wiley Online Library (wileyonlinelibrary.com).
DOI 10.1002/ajmg.a.34324

cluster, disrupted any known genes. They suggested that the three rearrangements disturb normal *HOXD* gene regulation by position effects. Yue et al. [2007] reported a boy with severe intellectual disability, funnel chest, bell-shaped thorax, and hexadactyly of both feet. The patient had a balanced de novo t(12;17)(p13.3;q21.3) translocation. The breakpoint was near the *HOXB* cluster. They proposed that misregulation of a *HOXB* gene(s) by position effect is responsible for the patient's phenotype. Jun et al. [2011] reported a patient with the *HOXA* cluster deletion with manifestations similar to those observed in hand-foot-genital syndrome, which is caused by a haploinsufficiency of *HOXA13*.

We report on a patient with distinctive skeletal anomalies with a submicroscopic deletion of 12q13. He was haploinsufficient for the *HOXC* gene cluster. So far, no human genetic disorders due to *HOXC* abnormalities are reported. We discuss the clinical features in the patient and the haploinsufficiency of the *HOXC* genes.

CLINICAL REPORT

The 14-year-old male propositus was the first-born child of a 26-year-old mother and a 30-year-old father, both healthy and non-consanguineous. After an uncomplicated pregnancy, he was born at 39 weeks of gestation by induced delivery. His length was 53 cm (90th centile). His birth weight was 3,010 g, within normal limits (25th centile). After birth, cardiac murmur was noticed. Echocardiography revealed tetralogy of Fallot. Cardiac surgery was carried out successfully at 2 years of age. Surgery for bilateral inguinal hernia and strabismus was done at 3 years of age. His dentition was abnormal. Persistent teeth erupted before the loss of primary teeth. He showed hypodontia.

His development was delayed since early infancy. From the age of 6 months, he received physical training for delayed motor development. He was able to roll over at 10 months of age, and to sit alone at 3 years of age. He started to walk independently at 5 years of age and the spine deformity appeared. His global development quotient was 20 at 3 years of age. He attended special education in school. Gradually, he could understand simple words. His intellectual quotient remained around 30 and verbal production was almost absent. However, recently he could express simple sentences using key boards.

Physical examination identified dysmorphic features, including a long face, a broad nose, prominent ears, bilateral low-set ears, downslanting palpebral fissures and a high palate. Severe kyphosis and mild scoliosis were remarkable features. The radial heads were dislocated bilaterally. Camptodactyly of middle and ring fingers, inflexible distal interphalangeal joints of index fingers and adducted thumbs of both hands were noted (Fig. 1A). Hearing and visual acuity were normal. His weight was 29 kg (<3rd centile), and his length was 160 cm (<3rd centile). His head circumference was average for his age, 14 years.

Radiographic analysis revealed severe kyphosis and mild scoliosis in the thoracic spine (Fig. 2A,B). The upper thorax was mildly narrowed. The proximal interphalangeal joints of both the middle and ring fingers showed flexion contracture with para-articular swelling (Fig. 1B). The proximal interphalangeal joints of both index fingers were swollen as well. The metacarpophalangeal joint of the right index finger and proximal interphalangeal joint of the left little finger showed ulnar deviation. The metacarpals were mildly undertubulated. Radiologic features of the fingers were like those seen in multiple synostosis syndrome. However, no carpal or tarsal coalition was found.

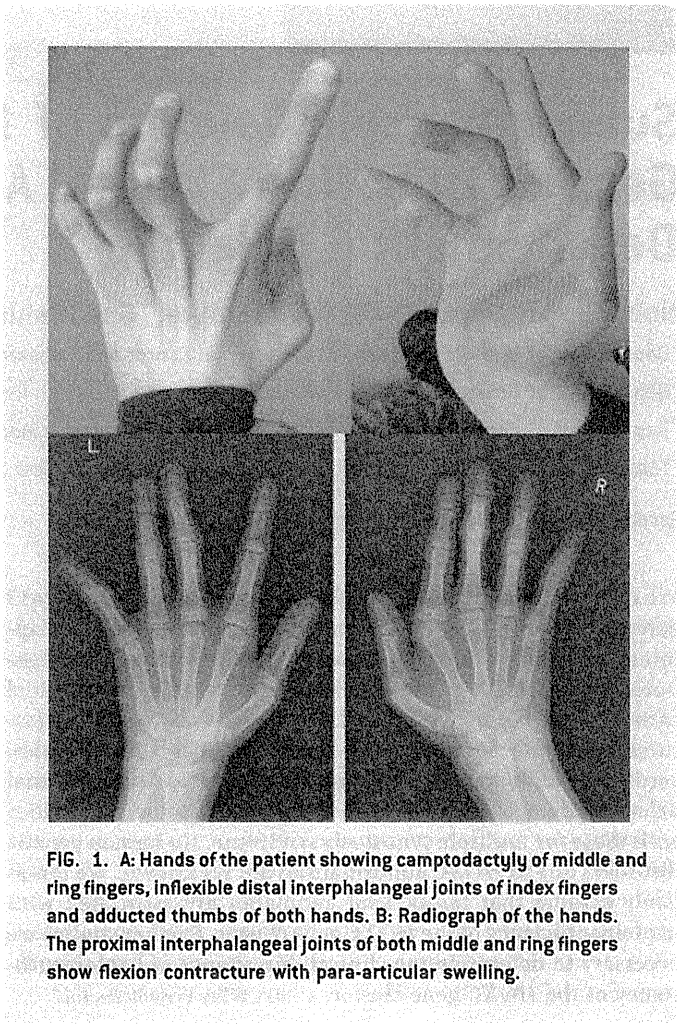

FIG. 1. A: Hands of the patient showing camptodactyly of middle and ring fingers, inflexible distal interphalangeal joints of index fingers and adducted thumbs of both hands. B: Radiograph of the hands. The proximal interphalangeal joints of both middle and ring fingers show flexion contracture with para-articular swelling.

Results of neuroradiological examinations including brain CT and MRI were normal. Routine laboratory tests were normal. His karyotype by G-banded analysis was 46,XY. Array-CGH analyses were performed to look for submicroscopic chromosomal aberrations.

MATERIALS AND METHODS

After obtaining informed consent and the permission of the institution's ethics committee, peripheral blood samples were drawn from the patient and his parents. Genomic DNA was extracted using the QIAquick DNA extraction kit (Qiagen, Valencia, CA).

Based on the hypothesis that the patient might have submicroscopic chromosomal aberrations, array-CGH analysis was performed using the Human Genome CGH Microarray 60K (Agilent Technologies, Santa Clara, CA) as described previously [Shimojima et al., 2009].